Towards the Clinical Implementation of Navigated Liver Ablation

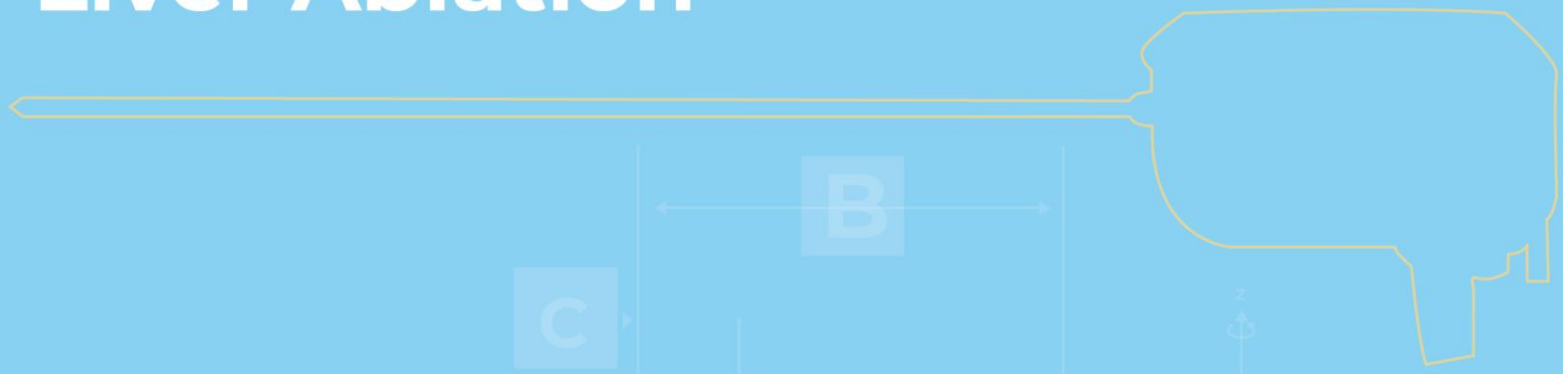

A thesis submitted to the Delft University of Technology, the Erasmus University Rotterdam and the Leiden University in partial fulfillment of the requirements for the degree of

Master of Science in Technical Medicine
Track Imaging & Intervention

by
Karin Antoinette Olthof

Universiteit Leiden

TU Delft Delft University of Technology

Erasmus Universiteit Rotterdam

Towards the Clinical Implementation of Navigated Liver Ablation

Karin Olthof

Student number : 4376013

12-07-2021

Thesis in partial fulfilment of the requirements for the joint degree of Master of Science in

Technical Medicine

Leiden University ; Delft University of Technology ; Erasmus University Rotterdam

Master thesis project (TM30004 ; 35 ECTS)

Dept. of Biomechanical Engineering, TUDELFT
January 2021 – July 2021
Supervisor(s):
Prof. dr. T.J.M. Ruers
Dr. M. Fusaglia
Drs. J.N. Smit

Thesis committee members:

Prof. dr. ir. Jaap Harlaar, TU Delft (chair)
Prof. dr. T.J.M. Ruers NKI-AvL
Dr. O. Ivashchenko LUMC

Universiteit Leiden

TU Delft Delft University of Technology

ERASMUS UNIVERSITEIT ROTTERDAM

Abstract

Surgical ablation is a well-accepted treatment for liver malignancies due to its ability to preserve the surrounding healthy liver tissue as opposed to surgical resection. Precise intraoperative localization of the lesion and correct needle placement are crucial factors for complete tumor ablation. These are difficult tasks due to interpatient variability and technical limitations of current technologies. Surgical navigation provides a live virtual representation of the surgery by showing the position of surgical instruments with respect to the critical anatomy. Navigation can improve tumor localization during surgical resection and it is therefore expected to similarly improve tumor ablation. The development and the clinical implementation of surgical navigation for hepatic tumor ablation were therefore explored in this thesis. A sterilizable adapter was developed carrying an electromagnetic (EM) sensor. This adapter is attachable to the ablation needle in order to track the surgical instrument. The tracking accuracy for this adapter calculated with respect to an EM tracked calibrated block was comparable to the Aurora 6DOF probe, a pointer currently used in the standard workflow of surgical navigations. With the use of this adapter, a virtual representation of the ablation needle could be presented to the surgical team. The workflow for navigated liver ablation was tested intraoperatively by three hepatobiliary surgeons. A cross-hair (i.e., bullseye) view was preferred by the surgeons to guide the ablation needle to the center of the target lesion. In this view, the tumor was visualized as if looking through the tip of the ablation needle. With the system usability score (SUS) of 65, refinement of the software visualization was indicated. Nonetheless, the surgeons want to use the system frequently and responded that it aided in localizing tumor(s), reducing complications, obtaining negative ablation margins and increasing certainty in decisions and actions. Next, a method for validation of the needle tip tracking accuracy at final needle placement was proposed and showed a mean accuracy of 2.2 mm in phantom experiments.

In conclusion, a workflow for open navigated liver ablation was developed and the first in vivo experiments have been performed which showed promising results. Intraoperative validation will be performed on 28 patients.

Acknowledgements

In the first place I would like to thank Matteo Fusaglia and Jasper Smit for welcoming me back after my ten week internship last summer and for helping me to define a thesis project that kept me enthusiastic up until the very last moment. Matteo, you could clarify complex matters for me, occasionally even by asking the right questions and you were always approachable for which I am grateful. Throughout my internship Jasper has shown me what it entails to work as a bridge between the medical and technical expertise. Thank you for sharing your experiences and knowledge of surgical navigation and for your enthusiasm and positivity. Additionally, I would like to express my gratitude to my clinical supervisor professor Theo Ruers for his knowledge, for keeping the clinical end goal in mind and for steering my research in the most promising direction. A critical view was provided during the meetings of the ultrasound liver navigation group at our institute by Sasha Ivashchenko, whom I would like to sincerely thank for being on my assessment committee.

Furthermore, I would like to thank Koert Kuhlmann and Niels Kok for their clinical feedback on my research and for being open and enthusiastic for technical innovations within the surgical field. At last, a special thanks to my beloved colleagues on the vide and the implementation team. You were always there for a quick brainstorm, the sometimes well-deserved distractions and the occasional drinks on Fridays. Without you, it would not have been the same.

Delft, June 2021 Karin Olthof

Contents

List of Figures

List of Abbreviations

Abbreviation	Definition
CSD	Central Sterilization Department
CT	Computed tomography
DLM	Disappearing liver metastases
DOF	Degrees of freedom
EBRT	External beam radiotherapy
EM	Electromagnetic
ETZ	Elisabeth-TweeSteden Hospital
FDG-PET	Fluorodeoxyglucose positron emission tomography
HCC	Hepatocellular carcinoma
HFJV	High Frequency Jet Ventilation
IOUS	Intra-operative ultrasound
IPA	Isopropyl Alcohol
IR	Infrared
LTP	Local tumor progression
LUS	Laparoscopic ultrasound
MI	Minimal invasive
MRI	Magnetic Resonance Imaging
MWA	Microwave ablation
NET	Neuroendocrine
NKI-AvL	Netherlands Cancer Institute – Antoni van Leeuwenhoek
OR	Operating room
PRISMA	Preferred Reporting Items for Systematic Reviews and Meta-Analyses
RFA	Radiofrequency ablation
SBRT	Stereotactic body radiation therapy
SCU	System Control Unit
SD	Standard deviation
SLA	Stereolithography
SIRT	Selective internal radiation therapy
SIU	Sensor Interface Unit
STL	Surface Tessellation Language
SUS	System Usability Scale
TPE	Target positioning error
US	Ultrasound
UV	Ultraviolet

Chapter 1

Introduction

1.1 Liver Cancer

Liver cancer is the sixth most common cancer and the second leading cause of cancer deaths in the world [1]. Liver cancer can be divided in two types: primary and secondary liver cancer (i.e., hepatic metastasis). The incidence of primary liver cancer in the Netherlands is approximately 800 per year, of which hepatocellular carcinoma (HCC) accounts for 80-85% of primary liver cancer [2,3]. More common are liver metastases, among which colorectal liver metastases are the most frequent due to their spread via the portal circulation [4,5]. Annually, over 14.000 patients are diagnosed with colorectal cancer in the Netherlands [6]. Up to 70% of these patients will develop liver metastases [7].

1.1.1 Diagnosis

Diagnosis of liver cancer consists of an extensive medical history, physical and radiological examination, blood tests and pathological assessment. Many patients who develop primary liver cancer are familiar with long-standing cirrhosis or other diseases that affect the liver functionalities, such as chronic hepatitis [8]. In these patients, rapid development of clinical features such as weight loss, malaise, jaundice and upper abdominal pain is suggestive for HCC. Physical examination can show an enlarged, irregular and tender liver. Serum α-fetoprotein, a tumor marker for the liver, may be raised but is normal in at least a third of patients [9].
Radiological investigation of primary liver cancer is performed using ultrasound (US), which has a sensitivity of 65 to 80% and a specificity of more than 90% [10]. As lesion size and presence of cirrhosis highly influence the sensitivity of US detection, computed tomography (CT) or magnetic resonance imaging (MRI) are often acquired to confirm the diagnosis in patients with suspected lesions on US [10,11]. CT or MRI is also preferred to determine the relation between the tumor and the surrounding critical anatomy. In the case of liver metastases, contrast-enhanced CT is acquired to localize the primary tumor. With a primary cancer of the gastrointestinal tract, lung, advanced breast cancer and lymphoma, there is a high incidence of liver metastases at the time of diagnosis [12]. For these patients, it is therefore advised to perform extensive examination of the liver. To improve the contrast-to-noise ratio between healthy liver tissue and malignant lesions on CT, iodine contrast is routinely used. Fluorodeoxyglucose positron emission tomography (FDG-PET) in combination with CT can be performed, to screen for extrahepatic tumor activity. MRI is often additionally acquired, as it offers the highest sensitivity to detect liver lesions, especially in small liver lesions (Ø<1 cm) [13]. At the Netherlands Cancer Institute – Antoni van Leeuwenhoek (NKI-AvL) diagnostic MR scans are performed using multi-phase MR sequences with a liver-specific gadolinium-based contrast agent. The multiphase 10 ml Gd-EOB-DTPA (Primovist, Bayer AG, Germany)-enhanced mDIXON sequence was optimized at this institute [14]. This scan can visualize the complete hepatic vasculature and biliary tree anatomy within one scan and allows for early detection of liver malignancies. Primovist is the standard MRI contrast agent used at the NKI-AvL for all liver metastases, except for neuroendocrine (NET) tumors, whereas Dotarem contrast is used.

1.1.2 Treatment Options

As for most cancers, the site and stage of the tumor determine the choice of treatment in liver cancer. Treatment options include radiation, chemotherapy, surgery and local ablation.
Conventional external beam radiotherapy (EBRT) can offer local control in unresectable HCC and palliation in the case of metastatic disease. However, it is not recommended for routine use, due to its major limitation of radiation-induced liver disease [15]. New emerging techniques such as stereotactic

body radiation therapy (SBRT) and selective internal radiation therapy (SIRT), in which cancer cells can be targeted more precisely and with a higher dose reduce this problem.
Systemic chemotherapy can be used in a palliative setting but also neoadjuvant to surgery. It increases survival in patients with a high risk of disease recurrence and can be used to render patients with unresectable disease eligible for resection by downstaging [16,17]. Most of the patients receiving systemic therapy additionally undergo local treatment.
Surgical resection is considered the gold standard for patients with primary or secondary liver lesions, as it is most effective in prolonging long-term survival [18,19]. Liver surgery is based on the anatomic description of the eight functional segments, first described by the French surgeon and anatomist Claude Couinaud (Figure 1.1). Couinaud's segments are based on the blood supply via the hepatic artery and portal vein, its venous drainage via the hepatic veins, and its biliary drainage. The segments are functionally independent, allowing resection of segments without damaging other segments. The unique regenerative abilities of the liver enable resections of up to 80% of its volume [20]. Nevertheless 70 to 80% of all patients with hepatic malignancies are not eligible for surgical resection [21,22]. Reasons for irresectability include resection not being technically feasible with tumor-free margins and patients having significant medical comorbidities or poor performance status [23]. This has resulted in an increased interest in less invasive local treatment methods.

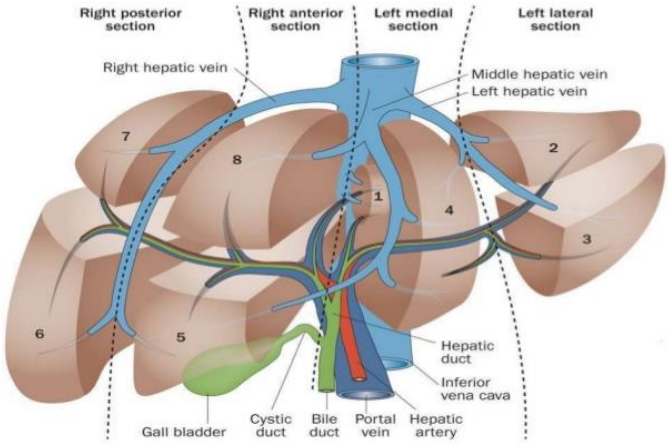

Figure 1.1: Couinaud's classification of liver segments [24]

Local ablative therapies have recently evolved to become a well-accepted treatment for liver malignancies. Liver ablation consists in applying a localized energy source or chemicals via needlelike applicators directly at the tumor, resulting in necrosis or apoptosis of tumor cells. The advantage of ablative techniques is its preservation of the surrounding healthy liver tissue. During thermal or cryogenic ablation, tissue is heated or cooled to cytotoxic levels (less than −40°C or more than 60°C) [25]. Different energy sources can be used, but the most mature and widely applied thermal ablation modalities for the treatment of liver lesions include radiofrequency and microwave energy, both used in the NKI-AvL.
Radiofrequency ablation (RFA) uses an alternating current of high energy radio waves. The current is conducted through the tissue via an ablation needle, causing perturbation of the ions present in the tissue around the electrode, resulting in frictional heat around the electrode (Figure 1.2a). When the tissue around the electrode is heated, it coagulates, thus losing its water content by the process of desiccation. This increases the tissue impedance causing the tissue to lose its ability to conduct the electrical current.
Microwave ablation (MWA) is based on electromagnetic waves in the microwave energy spectrum, which are shorter wavelengths and are emitted with a higher frequency than the radiofrequency waves. The microwaves cause dielectric heating, as the water molecules in tissue, which are natural dipoles, start vibrating and rotating with the changes of the electromagnetic field. The effect of MWA causes direct heating of a volume and is less reliant on conductive heating (Figure 1.2b). Therefore, MWA is faster and creates larger ablation zones compared to RFA. Also, MWA may be less susceptible to convective heat loss, and thus may be less prone to the heat-sink effect [26]. Heat-sink can occur when

ablating near large vessels, where the flowing blood sinks the heat from the tissue, countering the ablative effect.
There are several approaches for ablative therapy, including open, percutaneous, and laparoscopic approaches. Percutaneous ablations are performed by interventional radiologists, while open and laparoscopic ablations are carried out by hepatobiliary surgeons. Advantages of percutaneous liver ablation compared to the open approach include less invasiveness, less complications, reduced postoperative pain, shorter hospitalization and lower costs [27]. Compared to the surgical approach, percutaneous liver ablation is associated with higher recurrence rates of up to 60% [28]. Open surgical liver ablation is performed when other abdominal procedures are indicated, as it is often combined with liver or colorectal resection. Other indications for the open surgical approach are an increased risk of thermal injury to adjacent organs or bile ducts, or non-accessibility of the tumor percutaneously, as laparotomy provides the advantages of organ mobilization, tactile feedback and vascular control [29].

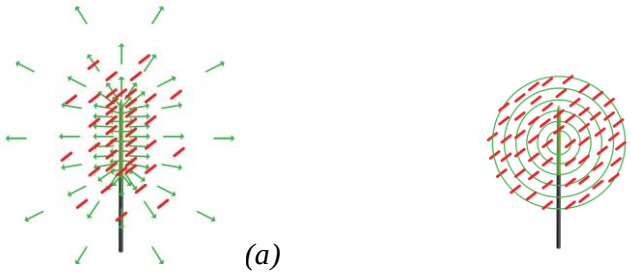

Figure 1.2: Spread of heat through tissue shown in red during (a) radiofrequency ablation and (b) microwave ablation [30]. The green arrows in (a) indicate the distribution of the radio waves that are stopped by the tissue, which causes frictional heating. The green circles in (b) indicate the electromagnetic field that causes water molecules to rotate, which causes heating.

1.1.3 Thesis Rationale

The prerequisites to achieve complete tumor ablation are precise intraoperative localization and accurate needle placement [31,32]. These are difficult tasks due to interpatient variability and technical limitations of current technologies.
US, for example, whilst being the standard modality for image guidance during liver surgery [33,34], suffers from several shortcomings (e.g., low resolution, suboptimal orientation by two-dimensional (2D) imaging, tissue echogenicity) which limit its effectiveness in discriminating between tumor and healthy tissue [35,36]. Another important challenge is the localization of very small or vanishing lesions after positive response of neo-adjuvant systemic treatment [37]. Even in the case of radical radiologic response, microscopically residual disease is still present in up to 80% of the disappeared liver metastases [38], and therefore have to be surgically treated, often with ablation.
Surgical navigation provides a live virtual representation of the surgery by showing the position of surgical instruments with respect to the critical anatomy. This has been shown to improve tumor localization during surgical resection. Similar improvements can be transferred in the context of tumor ablation. This thesis explores the development and the clinical implementation of surgical navigation for hepatic tumor ablation.

1.2 Image-Guided Liver Surgery

At this institute, the surgeon is provided with a patient-specific 3D model of the liver, its vascular and biliary anatomy and the tumors, based on preoperative imaging [39]. This model can be used prior to the surgery for surgical planning, but is also provided during the surgery on a tablet computer enclosed in a sterile cover. Interactive 3D models give a more intuitive assessment of the patient-specific anatomy compared to conventional imaging and can assist in the decision-making process [39]. During image-guided surgery (i.e. surgical navigation) this is taken a step further and the 3D planning is matched to the intra-operative anatomical situation using a tracked US probe. This matching process is called registration, and it aims at determining a geometrical mapping between the preoperative imaging and

the intraoperative organ position. After registration, surgical instruments can be tracked to visualize their orientation and position with respect to the patient's anatomy. In this way, the surgeon can be guided towards the tumor(s).

1.2.1 3D Modeling

The preoperative 3D models of the liver are generally made based on the diagnostic MR scans performed with the multiphase mDIXON sequence. An algorithm for automated segmentation of the liver surface, hepatic vasculature and biliary tree anatomy of these specific MR images was created and integrated into an extension of 3D Slicer (BWH, https://www.slicer.org/) by Ivashchenko et al. [14]. Nonetheless, it is also possible to make the preoperative models based on contrast-enhanced CT or MR scans with different scanning protocols/sequences. The obtained segmentations from the automated segmentation pipeline are assessed and manually adjusted if necessary and additionally tumor contours are manually added to the segmentation using the Editor segmentation module of 3D Slicer. The resulting patient-specific 3D models, as shown in Figure 1.3, are used for navigation.

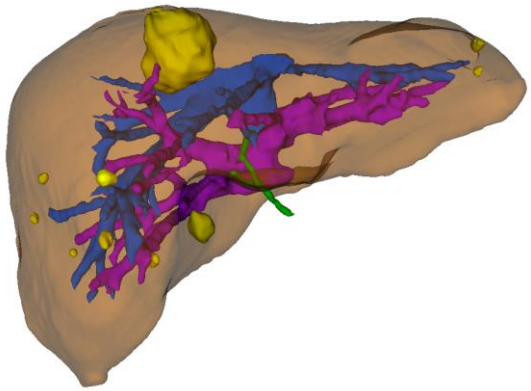

Figure 1.3: Example of a 3D liver model, including the hepatic veins (blue), portal veins (purple), bile ducts (green) and lesions (yellow).

1.2.2 Instrument Tracking

Tracking links the preoperative 3D model with the real-time intraoperative situation and determines the location and orientation of the surgical instruments. It can be performed either optically or electromagnetically (EM).
Active optical tracking uses cameras to determine the position and orientation of flashing light emitting diodes, which can be mounted on surgical instruments. More common however is passive optical tracking, which relies on camera systems that emit and detect near infrared (IR) light. Instruments are equipped with retro-reflective markers, which reflect the incoming light back to the cameras. The reflections are detected by the cameras and the position determined through triangulation. These systems are wireless but require direct sight between the retro-reflective markers and the cameras [40].
EM tracking consists of a field generator, control electronics and EM sensors. Two types of field generators are used at this institute: the Aurora planar 20-20 field generator and the Aurora tabletop field generator (Northern Digital Inc. (NDI), Waterloo, Ontario, Canada). The planar field generator (Figure 1.4) is mounted on a flexible positioning arm, which can be placed in proximity to the patient's head. The tabletop field generator (Figure 1.5) is mounted underneath the surgical bed. During the surgery, the field generator emits an EM field of a known geometry. Unique voltages are induced within the sensors, when these are placed within this EM field. These voltages are amplified and digitized by the Sensor Interface Unit (SIU). The amplified signal is in its turn detected by the System Control Unit (SCU), which calculates the position and orientation of the sensors and passes this information on to the host computer [41]. The main drawback of EM tracking is its sensitivity to interference of large ferromagnetic objects nearby the field generator, distorting the magnetic field and affecting the tracking accuracy [42,43].

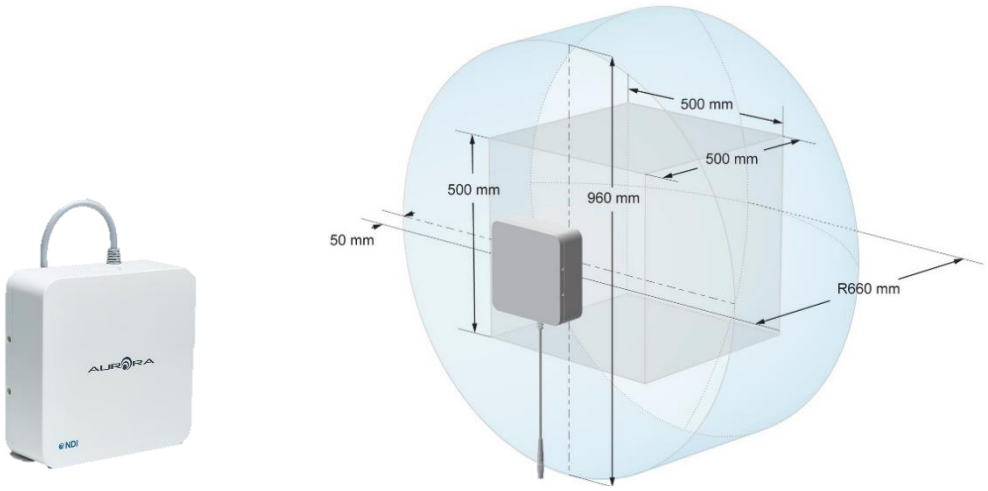

Figure 1.4: Aurora NDI planar 20-20 field generator, with its EM field [45].

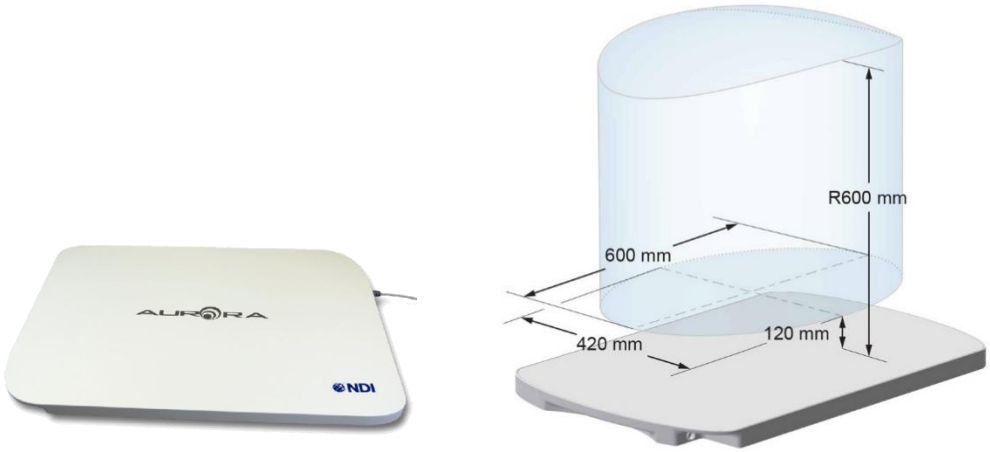

Figure 1.5: Aurora NDI tabletop field generator, with its EM field [41].

There are two types of EM sensors, namely five degrees of freedom (5DOF) sensors and six degrees of freedom (6DOF) sensors. The 5DOF sensors provide three positions and two orientations while the 6DOF EM sensors provide an additional orientation (Figure 1.6). Hence, unique positions can be determined using one single 6DOF sensor or two combined 5DOF sensors [44].

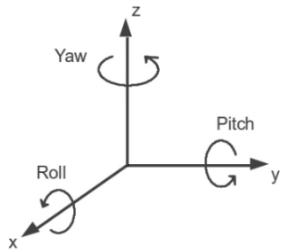

Figure 1.6: The six degrees of freedom in a Euclidean space: three translations (X,Y,Z) and three rotations (roll, pitch, yaw)

In the current surgical liver navigation workflow an US probe, a pointer and the liver surface are tracked. Real-time tracking of these elements is possible when the EM sensors are inside the EM field.
The pointer used is the Aurora 6DOF Probe (NDI, Waterloo, Ontario, Canada) (Figure 1.7a). The intraoperative I14C5T ultrasound transducer by BK (BK Medical, Peabody, MA, USA) is tracked using a custom-made, 3D-printed adapter containing an EM sensor (Figure 1.7b). This adapter has a unique positioning on the US probe, for which it is calibrated. At last, after the laparotomy, a sterilized sensor (Figure 1.7c) is attached to the liver (segment IV or V) in close proximity to the targeted lesion with a

medical adhesive. This sensor is used to track the location of the liver during intraoperative movements of the organ.
A goal for this thesis is to track aside from the liver, a pointer and the US, an ablation needle that can be used during open liver ablation.

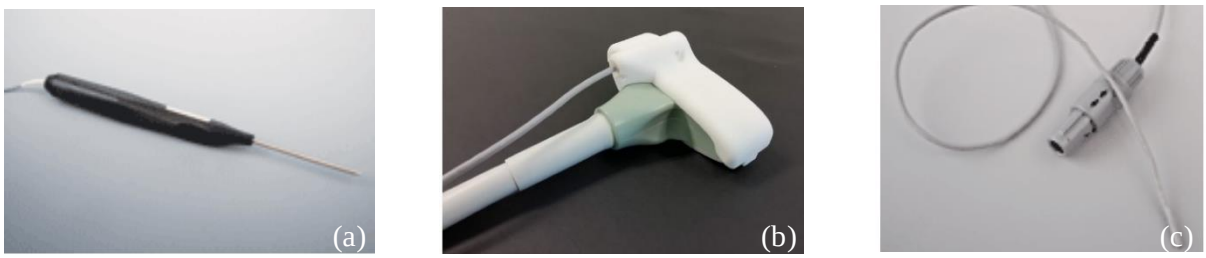

Figure 1.7: Tracked instruments surgical liver navigation workflow: (a) the Aurora 6DOF Probe, (b) the custom-made adapter for BK US probe, and (c) the Aurora 6DOF Cable Tool used for attachment to the liver surface.

1.2.3 Registration

In the context of surgical navigation, registration is the geometrical mapping between different coordinate systems. In the case of navigated liver surgery at the NKI-AvL, a registration is necessary between two different imaging modalities: the preoperative imaging and the intra-operative US (IOUS) visualizing the organ position and orientation during the surgery. This is because the origin of the coordinates system and orientation of the axes of the preoperative scan and the IOUS are different. We aim to obtain a correspondence between pixel positions in the ultrasound images ${}^{US}p$ and voxel positions within the MR (or CT) volume ${}^{MR}p$.
The calibration transformation from the 2D US image to the tracked US probe can be denoted as ${}^{Probe}T_{US}$. Consequently, the tracked probe is detected by the EM field generator, resulting in the transformation ${}^{EM}T_{Probe}$. However, the liver is a highly deformable organ especially after laparotomy. Therefore, placement of an electromagnetic sensor is required to compensate for the movements of the liver caused by surgical manipulation and respiration. A reference sensor is attached to the liver surface. This marker can be placed close to a liver metastasis, therewith enabling to track the local movement of the metastatic lesion during surgery. The relation between the tracked probe and the reference sensor is established by continuously updating the transformation matrix ${}^{EM}T_{Probe}$. Image registration is finally performed by linking the preoperative imaging to the EM field (${}^{MR}T_{EM}$). An overview of the steps of the aforementioned registration is shown in Figure 1.8. Formula 1.1 shows the transformation of a point ${}^{US}p$, to the registered point ${}^{MR}p$ in the preoperative scan.

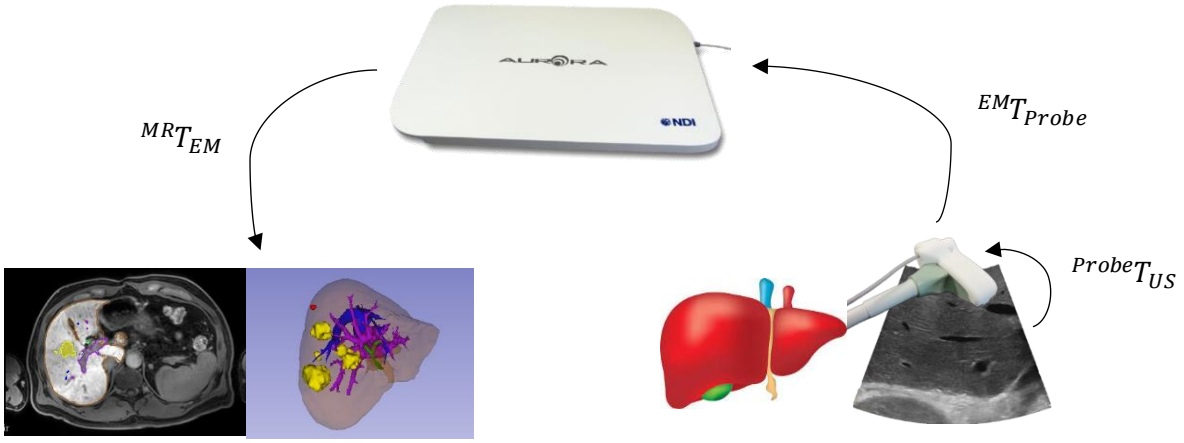

Figure 1.8: Overview of steps taken for registration from preoperative imaging modality to intra-operative US.

$$^{MR}p = {}^{MR}T_{EM} \cdot {}^{EM}T_{Probe} \cdot {}^{Probe}T_{US} \cdot {}^{US}p \quad (1.1)$$

To determine $^{MR}T_{EM}$ and to align the two modalities, mutual information from the US and preoperative image is required. Since hepatic vessels are prominent structures in both preoperative imaging and intraoperative US imaging, most registration methods rely on those. Two different registration methods are investigated in ongoing research of the N18ULN study at the NKI-AvL. In phase I of this study, landmark-based registration is performed. Vascular bifurcations (the location where a vessel splits) are identified by the surgeon on IOUS and matched using rigid registration to the corresponding points on the preoperative 3D model.
In phase II of the study, vessel segmentations of the IOUS and preoperative model are registered. Firstly, an electromagnetically tracked ultrasound sweep of the patient's liver takes place in close proximity to the targeted lesion. During this ultrasound sweep, 2D US images from the transducer are stored, and used for an automatic reconstruction of a 3D US volume in the navigation software. In this 3D volume, vessels are segmented automatically and centerlines of the vessels are extracted, which are then used for deformable registration to the preoperative scan. An overview of this workflow is shown in Figure 1.9. Accuracy of the registration is verified during surgery based on visual inspection of the registered volumes by the surgeon and the researcher. After the surgery the accuracy of the registration is additionally determined by calculating the distance from the center of the registered target lesion to its alias in the 3D US volume.
Within the approval by the Medical Ethics Review Committee (METC) for the N18ULN study, consent was also obtained to evaluate feasibility and accuracy of real-time electromagnetic tracking of MWA needles during ablations of liver lesions in open surgery. Before navigated ablation is possible, a registration method such as or comparable to the methods previously used in within this study, is necessary.

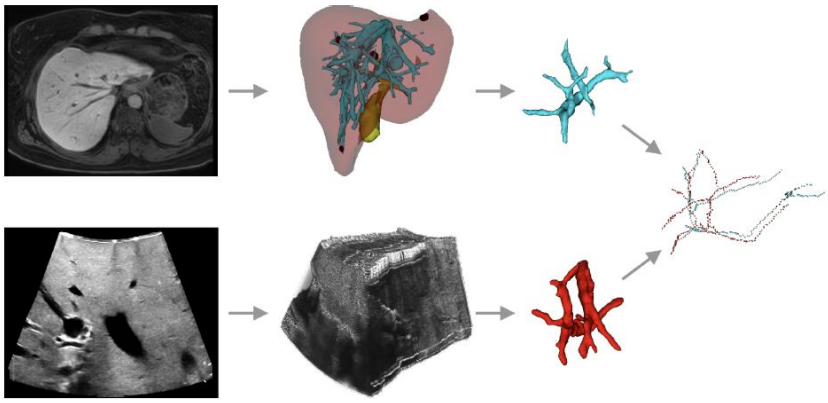

Figure 1.9: Vasculature is extracted from the preoperative scan prior to surgery. During surgery vasculature is extracted from a reconstructed US volume. Centerlines from both modalities are used for registration. [45]

1.3 Objectives

The objective of this thesis is to provide a complete surgical workflow for electromagnetically tracked open liver ablation at the NKI-AvL. Several subgoals can be defined to achieve this objective, taking into account the current workflow for navigated liver surgery at this institute. These subgoals are listed below:

1. Development of a method for tracking of the ablation needle (Chapter 3).
2. Making necessary software alterations for intra-operative visualization (Chapter 4).
3. Development of a validation method for the intraoperative tracking accuracy for navigated ablation (Chapter 5).

References

1. Ferlay J, Soerjomataram I, Dikshit R, Eser S, Mathers C, Rebelo M, Parkin DM, Forman D, Bray F. Cancer incidence and mortality worldwide: sources, methods and major patterns in GLOBOCAN 2012. Int J Cancer 2015; 136: E359-E86.
2. Integraal Kankercentrum Nederland. *Incidentie HPB-tumoren*. 2019. URL: https://www.iknl.nl/kankersoorten/hpb-tumoren/registratie/incidentie.
3. Bosch, F. X., Ribes, J., & Borràs, J. (1999). Epidemiology of primary liver cancer. In Seminars in liver disease (Vol. 19, No. 03, pp. 271-285). © 1999 by Thieme Medical Publishers, Inc..
4. Ananthakrishnan, A., Gogineni, V., & Saeian, K. (2006, March). Epidemiology of primary and secondary liver cancers. In Seminars in interventional radiology (Vol. 23, No. 01, pp. 047-063). Copyright© 2006 by Thieme Medical Publishers, Inc., 333 Seventh Avenue, New York, NY 10001, USA..
5. Peterhans, M., vom Berg, A., Dagon, B., Inderbitzin, D., Baur, C., Candinas, D., & Weber, S. (2011). A navigation system for open liver surgery: design, workflow and first clinical applications. *The international journal of medical robotics and computer assisted surgery*, *7*(1), 7-16.
6. Integraal Kankercentrum Nederland. *Incidentie darmkanker*. 2019. URL: https://www.iknl.nl/kankersoorten/darmkanker/registratie/incidentie
7. Van de Velde, C. J. H. (2005). Treatment of liver metastases of colorectal cancer. *Annals of oncology*, *16*, ii144-ii149.
8. Janevska, D., Chaloska-Ivanova, V., & Janevski, V. (2015). Hepatocellular carcinoma: risk factors, diagnosis and treatment. *Open access Macedonian journal of medical sciences*, 3(4), 732.
9. Kumar, P. J., & Clark, M. L. (2002). *Kumar & Clark clinical medicine*. Edinburgh: Saunders.
10. Andreana, L., Isgrò, G., Pleguezuelo, M., Germani, G., & Burroughs, A. K. (2009). Surveillance and diagnosis of hepatocellular carcinoma in patients with cirrhosis. *World journal of hepatology*, 1(1), 48.
11. Oliva, M. R., & Saini, S. (2004). Liver cancer imaging: role of CT, MRI, US and PET. Cancer imaging, 4(Spec No A), S42.
12. Robinson, P. J. (2002). The early detection of liver metastases. Cancer Imaging, 2(2), 1-3.
13. Floriani, I., Torri, V., Rulli, E., Garavaglia, D., Compagnoni, A., Salvolini, L., & Giovagnoni, A. (2010). Performance of imaging modalities in diagnosis of liver metastases from colorectal cancer: a systematic review and meta-analysis. *Journal of Magnetic Resonance Imaging*, 31(1), 19-31.
14. Ivashchenko, O. V., Rijkhorst, E. J., Ter Beek, L. C., Hoetjes, N. J., Pouw, B., Nijkamp, J., ... & Ruers, T. J. (2020). A workflow for automated segmentation of the liver surface, hepatic vasculature and biliary tree anatomy from multiphase MR images. *Magnetic resonance imaging*, 68, 53-65.
15. Chen, C. P. (2019). Role of radiotherapy in the treatment of hepatocellular carcinoma. *Journal of clinical and translational hepatology*, *7*(2), 183.
16. Liu, W., Zhou, J. G., Sun, Y., Zhang, L., & Xing, B. C. (2016). The role of neoadjuvant chemotherapy for resectable colorectal liver metastases: a systematic review and meta-analysis. *Oncotarget*, 7(24), 37277.
17. Leonard, G. D., Brenner, B., & Kemeny, N. E. (2005). Neoadjuvant chemotherapy before liver resection for patients with unresectable liver metastases from colorectal carcinoma. *Journal of Clinical Oncology*, 23(9), 2038-2048.
18. Gallinger, S., Biagi, J. J., Fletcher, G. G., Nhan, C., Ruo, L., & McLeod, R. S. (2013). Liver resection for colorectal cancer metastases. *Current Oncology*, 20(3), e255.
19. Gena P Kanas, Aliki Taylor, John N Primrose, Wendy J Langeberg, Michael A Kelsh, Fionna S Mowat, Dominik D Alexander, Michael A Choti, and Graeme Poston. Survival after liver resection in metastatic colorectal cancer: review and meta-analysis of prognostic factors. *Clinical epidemiology*, 4:283, 2012.

20. Guglielmi, A., Ruzzenente, A., Conci, S., Valdegamberi, A., & Iacono, C. (2012). How much remnant is enough in liver resection?. *Digestive surgery*, 29(1), 6-17.
21. PC Simmonds et al. "Surgical resection of hepatic metastases from colorectal cancer: a systematic review of published studies". In: *British journal of cancer* 94.7 (2006), p. 982.
22. Glassberg, M. B., Ghosh, S., Clymer, J. W., Wright, G. W., Ferko, N., & Amaral, J. F. (2019). Microwave ablation compared with hepatic resection for the treatment of hepatocellular carcinoma and liver metastases: a systematic review and meta-analysis. *World journal of surgical oncology*, 17(1), 98.
23. Takahashi, H., & Berber, E. (2020). Role of thermal ablation in the management of colorectal liver metastasis. *Hepatobiliary Surgery and Nutrition*, 9(1), 49.
24. ITLS. *Couinaud's Segmental Anatomy of the Liver and Proposed Classification of Pediatric Liver Tumors*. (2021). URL: https://ilts.org/insights/couinauds-segmental-anatomy-of-the-liver-and-proposed-classification-of-pediatric-liver-tumors/.
25. Knavel, E. M., & Brace, C. L. (2013). Tumor ablation: common modalities and general practices. *Techniques in Vascular & Interventional Radiology*, 16(4), 192-200.
26. Wells, S. A., Hinshaw, J. L., Lubner, M. G., Ziemlewicz, T. J., Brace, C. L., & Lee, F. T. (2015). Liver ablation: best practice. *Radiologic Clinics*, 53(5), 933-971.
27. Crucitti, A., Danza, F. M., Antinori, A., Vincenzo, A., Pirulli, P. G., Bock, E., & Magistrelli, P. (2003). Radiofrequency thermal ablation (RFA) of liver tumors: percutaneous and open surgical approaches. *J Exp Clin Cancer Res*, 22(4 Suppl), 191-195.
28. Mulier, S., Ni, Y., Jamart, J., Ruers, T., Marchal, G., & Michel, L. (2005). Local recurrence after hepatic radiofrequency coagulation: multivariate meta-analysis and review of contributing factors. *Annals of surgery*, 242(2), 158.
29. Giglio, M. C., Logghe, B., Garofalo, E., Tomassini, F., Vanlander, A., Berardi, G., ... & Troisi, R. I. (2020). Laparoscopic versus open thermal ablation of colorectal liver metastases: a propensity score-based analysis of local control of the ablated tumors. *Annals of surgical oncology*, 1-11.
30. Joseph D. Brannan. Thermal Ablation: Understanding the Breakthrough to Predictability Spherical Ablations with the Thermosphere™ Technology. URL: http://medtronicsolutions.medtronic.com/ThermospherePaper
31. Simpson, A. L., & Kingham, T. P. (2016). Current evidence in image-guided liver surgery. *Journal of Gastrointestinal Surgery*, 20(6), 1265-1269.
32. Citone, M., Fanelli, F., Falcone, G., Mondaini, F., Cozzi, D., & Miele, V. (2020). A closer look to the new frontier of artificial intelligence in the percutaneous treatment of primary lesions of the liver. *Medical Oncology*, 37, 1-7.
33. Bao, P., Sinha, T. K., Chen, C. C., Warmath, J. R., Galloway, R. L., & Herline, A. J. (2007). A prototype ultrasound-guided laparoscopic radiofrequency ablation system. *Surgical endoscopy*, 21(1), 74-79.
34. Joo, I. (2015). The role of intraoperative ultrasonography in the diagnosis and management of focal hepatic lesions. *Ultrasonography*, 34(4), 246
35. Kingham, T. P., Scherer, M. A., Neese, B. W., Clements, L. W., Stefansic, J. D., & Jarnagin, W. R. (2012). Image-guided liver surgery: intraoperative projection of computed tomography images utilizing tracked ultrasound. *HPB*, 14(9), 594-603.
36. Kruskal, J. B., & Kane, R. A. (2006). Intraoperative US of the liver: techniques and clinical applications. *Radiographics*, 26(4), 1067-1084.
37. Perrodin, S., Lachenmayer, A., Maurer, M., Kim-Fuchs, C., Candinas, D., & Banz, V. (2019). Percutaneous stereotactic image-guided microwave ablation for malignant liver lesions. *Scientific reports*, 9(1), 1-8.
38. Kuhlmann, K., Van Hilst, J., Fisher, S., & Poston, G. (2016). Management of disappearing colorectal liver metastases. *European Journal of Surgical Oncology (EJSO)*, 42(12), 1798-1805.
39. Ivashchenko, O. V., Smit, J. N., Nijkamp, J., Ter Beek, L. C., Rijkhorst, E. J., Kok, N. F., ... & Kuhlmann, K. F. (2021). Clinical Implementation of In-House Developed MR-Based Patient-Specific 3D Models of Liver Anatomy. *European Surgical Research*, 1-10.

40. Poulin F, Amiot LP. Interference during the use of an electromagnetic tracking system under OR conditions. *J Biomechanics*. 2002;35(6):733–737.
41. NDI. *Aurora*. 2020. URL : https://www.ndigital.com/products/aurora/
42. Sindram, D., McKillop, I. H., Martinie, J. B., & Iannitti, D. A. (2010). Novel 3-D laparoscopic magnetic ultrasound image guidance for lesion targeting. *Hpb*, 12(10), 709-716.
43. Sadjadi H, Hashtrudi-Zaad K, Fichtinger G. Simultaneous electromagnetic tracking and calibration for dynamic field distortion compensation. *IEEE Trans Biomed Eng*. 2016;63(8):1771–1781.
44. Nijkamp, J., Schermers, B., Schmitz, S., de Jonge, S., Kuhlmann, K., van der Heijden, F., ... & Ruers, T. (2016). Comparing position and orientation accuracy of different electromagnetic sensors for tracking during interventions. International journal of computer assisted radiology and surgery, 11(8), 1487-1498.
45. Thomson, B.R. Automated vascular region segmentation in ultrasound to utilize surgical navigation in liver surgery. 2019. URL: https://essay.utwente.nl/79399/

Chapter 2

Navigation Based on 3D Models to Guide Liver Ablation: a Review of the State of the Art

Karin A. Olthof[(a)], Jasper N. Smit[(b)], Matteo Fusaglia[(b)], Theo J.M. Ruers[(b)]

[(a)] Student MSc Technical Medicine, Technical University Delft, Leiden University Medical Center and Erasmus Medical Center Rotterdam, the Netherlands.
[(b)] Department of Surgical Oncology, The Netherlands Cancer Institute, Amsterdam, The Netherlands

Abstract

Ablative therapies are increasingly used for the treatment of primary and secondary liver lesions. Currently, ultrasonography (US) is the most widely used imaging modality to guide open, laparoscopic and percutaneous hepatic ablation. Challenges to ultrasound guidance may arise due to its low resolution, suboptimal orientation by two-dimensional imaging and tissue echogenicity. Navigation, in which modalities such as ultrasound, computed tomography (CT) and magnetic resonance imaging (MRI) are combined with 3D models, could potentially resolve these challenges. This study provides a state-of-the-art review regarding the use of navigation based on preoperative 3D modelling in liver ablation with US as intraprocedural imaging modality.

Keywords: Image-guided surgery, surgical navigation, liver ablation.

2.1 Introduction

Surgical resection is considered the gold standard for patients with primary or secondary liver lesions [1,2]. However, 70 to 80% of all patients with hepatic malignancies are not eligible for surgical resection [3,4]. Possible reasons for irresectability include resection not being technically feasible with tumor-free margins and patients having significant medical comorbidities or poor performance status [5]. This has resulted in increased interest in less invasive procedures, such as local liver ablation [6].

Liver ablation consists in applying a localized energy source directly at the tumor. Different types of energy can be applied (e.g., microwave, radio, electricity, cryo-ablation) resulting in cell necrosis or apoptosis. The advantage of ablative techniques is the delivery of localized energy, therefore preserving the surrounding healthy liver tissue. There are several approaches for ablative therapy, including open, percutaneous, and laparoscopic approaches. Percutaneous ablations are performed by interventional radiologists, while open and laparoscopic ablations are carried out by hepatobiliary surgeons.

In liver ablation, the prerequisite to achieve complete tumor ablation is accurate needle placement [7]. Intraprocedural image guidance is crucial to successfully position the ablation needle and avoid damage of the vascular and biliary system [8,9]. Due to its availability, absence of ionizing radiation, real-time imaging possibilities and low costs, ultrasonography (US) is the most widely used guidance in open, laparoscopic and percutaneous hepatic ablation [10,11].

Nevertheless, standard US suffers from several shortcomings (e.g., low resolution, suboptimal orientation by two-dimensional (2D) imaging, tissue echogenicity) which limit its effectiveness in discriminating between tumor and healthy tissue [12,13]. Another important challenge in US imaging is the visualization of very small or vanishing lesions after complete response of neo-adjuvant systemic treatment [14]. Even in the case of radical radiographic response, microscopically residual disease is still present in up to 80% of the disappeared liver metastasis [15]. Thus, techniques are necessary to improve localization and ablation accuracy of hepatic tumors.

Virtual navigation, in which modalities such as ultrasound, computed tomography (CT) and magnetic resonance imaging (MRI) are combined with three-dimensional (3D) models, could potentially be the solution to these problems [16]. Methods of navigation for liver ablation can slightly vary, but the general principle consists of the display of the position of tracked instruments relative to a 3D model of the organ, based on preoperative CT and/or MRI images. During the procedure, this model is registered to the intraprocedural imaging modality, such as US, CT or MRI.

Intraprocedural CT or MRI devices are rarely available in common operating and intervention rooms (due to high costs, complicated integration in the clinical workflow and limited space), while US is the standard modality in liver ablation. In addition, re-registration of the liver position and orientation to the preoperative model is less cumbersome and time-consuming using US. Therefore, this research will focus on navigation systems which utilize US as intraprocedural imaging modality during open, minimal invasive (MI) and percutaneous ablation. Within the following sections, a review of the state of the art regarding the use of navigation based on preoperative 3D modelling in liver ablation will be provided.

2.2 Methods

A systematic review was conducted in accordance with the Preferred Reporting Items for Systematic Reviews and Meta-Analyses (PRISMA) guidelines [17].

Data was collected from the electronic database MEDLINE/PubMed up to the 14th of December 2020. No restrictions based on year of publication or study design were applied. The complete search strategy contains the following Mesh terms and keywords:
("Liver"[Mesh] OR "liver"[tiab] OR "hepatocellular"[tiab] OR "hepatic"[tiab]) AND ("Ablation Techniques"[Mesh] OR "ablation"[tw] OR "needle targeting"[tw]) AND ("navigat*"[tw] OR "image guid*"[tw]) AND ("ultrasound"[tw] OR "ultrasonography"[tw] OR "US"[tw]).*

Firstly, articles were screened on title and abstract by one independent reviewer. Articles were excluded if they were a review, individual case report, or did not cover navigated liver ablation.
Secondly, full text articles were examined by the same independent reviewer. Articles in which no 3D model creation of the liver is carried out, or articles in which intraprocedural registration is not performed on US or in which the method of intraprocedural registration is not mentioned were excluded. Articles were also excluded in which no ablation was performed using the navigation system, or if they were not available in English language. There were no publishing date limitations. In the event of multiple publications from the same center, patient populations were ensured not to overlap. The process of inclusion and exclusion is presented in the PRISMA flowchart in Figure 2.1.

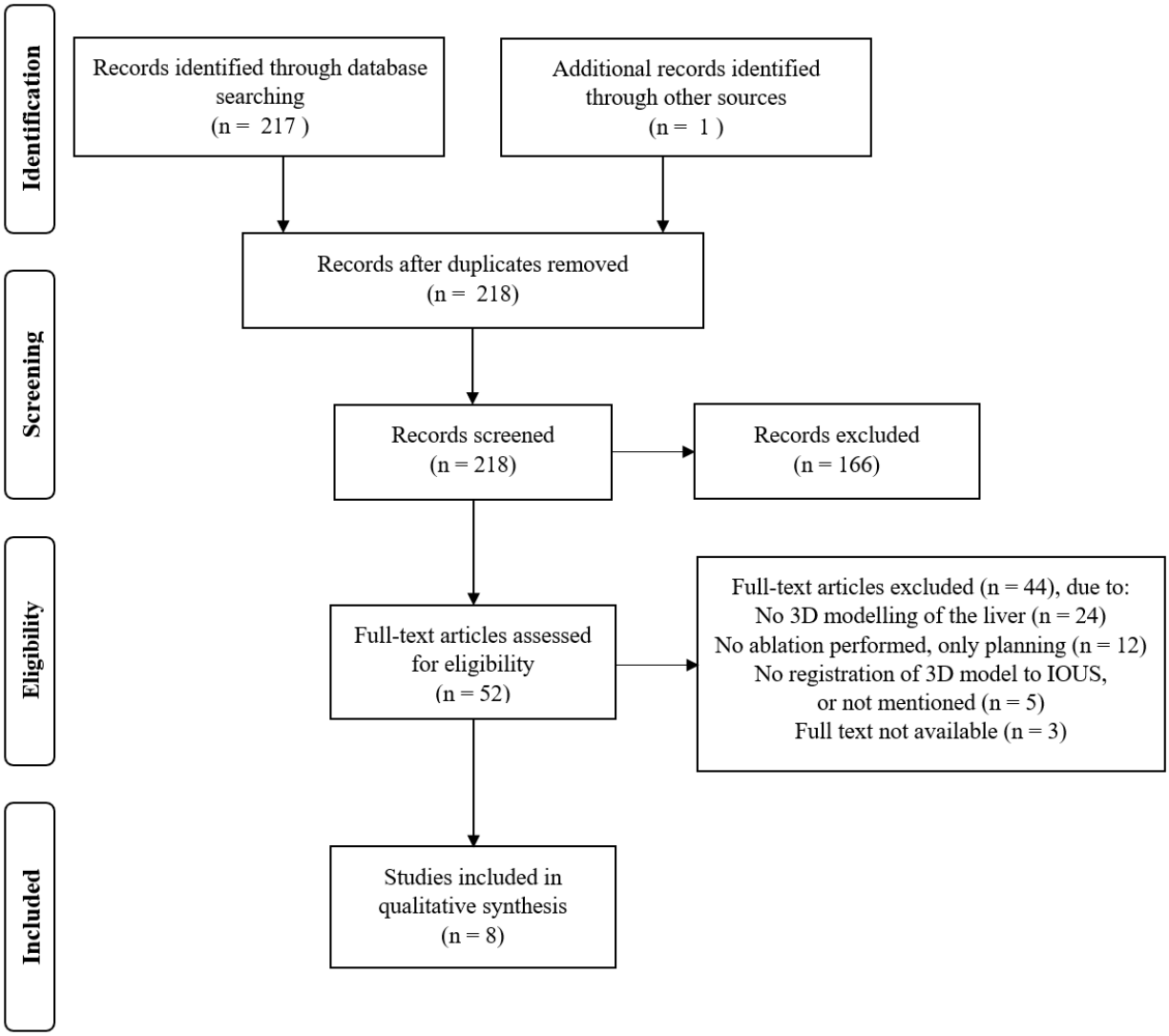

Figure 2.1: PRISMA flowchart included articles

Table 2.1: Non-clinical studies

References	Wu et al. [18]	Martin et al. [19]
Type of model	Animal	Phantom
Open (O)/Laparoscopic (L)/Percutaneous (P)	O	O
Ablation only (A), or in combination with resection (R)	A	A
N tumors per each liver model	4	7 (3 targeted US only, 4 3D guided)
N ablations performed	30 livers ablated by 5 interv. radiologists and 5 medical students	30 surgeons ablating 1 phantom
Preoperative imaging modality	CT	CT
Software for 3D modelling	Self-developed	MeVis Distant Services (MeVis Research, Bremen, Germany)
Tracking method	EM (Aurora, NDI)	Optical (Polaris Vicra, NDI)
Tracker location ablation needle	Stylet	Shaft
Navigation system	Self-developed	CAS-One (CAScination AG, Bern, Switzerland)
Registration method	Registration of eight fiducial markers of known location to the preoperative model.	Sweep of liver using tracked US probe, automatic vasculature segmentation in 3D US volume, and automatic alignment to 3D model.
Visualization	1. Real-time US imaging with needle trajectory. 2. Position and orientation of tracked instruments relative to 3D virtual model. 3. US-CT fusion image including needle trajectory.	1. Real-time US images with co-registered preoperative image data. 2. Position and orientation of tracked instrument relative to 3D virtual model. 3. 2D visualization of lateral and longitudinal displacement view relative to a selected target structure (e.g. a lesion).
Outcomes	Puncture accuracy conventional US and 3D guidance	Percentage of correctly identified lesions and puncture accuracy and time.
Conventional US detection rate	NA	73%
3D guidance detection rate	NA	100%
Puncture accuracy conventional US	Medical students: 7.7 ± 1.8 mm Interv. radiologist: 3.9 ± 0.9 mm	Puncture of center portion of target lesion in 65% of cases (error NA)
Puncture accuracy 3D guidance	Medical students: 2.7 ± 0.7 mm Interv. radiologist: 1.8 ± 0.5 mm	Puncture of center portion of target lesion in 95% of cases (error NA)

Table 2.2: Clinical studies

References	Kingham et al. [12]	Banz et al. [20]	Zhang et al. [21]	Kingham et al. [22]	Beerman et al. [23]	Pak et al. [24]
Type of study	Prospective	Retrospective	Retrospective	Prospective	Retrospective	Prospective
Ablation only (A), or also resection (R)	R	R	A	R	R	R
N patients/tumors receiving 3D guidance	3/NA	Phase 1: 8/NA Phase 2: 2/NA Phase 3: 17/NA	19/19	14/22	Open 29/281 Laparoscopic 79/438 Percutaneous 374/787	14/38
Patient age receiving 3D guidance	55 (46-65)	Phase 1: 59.3 ± 9.1 Phase 2: 61.1 ± 9.4 Phase 3: 60.2 ± 11.5	61.26 ± 9.86 (44–75)	53 (31-74)	NA	60 (30-76)
Open (O)/Laparoscopic (L)/Percutaneous (P)	O	O	P	O	All	O
Software 3D modelling	Scout™ Liver (Analogic)	MeVis Distant Services (MeVis Research, Bremen, Germany)	Self-developed by connecting open source libraries	NA	NA	NA
Tracking method	Optical (Polaris Spectra, NDI)	Optical (Polaris Vicra, NDI)	EM (Aurora, NDI)	Optical (Polaris Spectra, NDI)	Optical (Polaris Vicra, NDI)	Optical (Polaris Spectra, NDI)
Tracker location ablation needle	Shaft	Shaft	Shaft	NA	NA	No ablation probe tracker
Navigation system	Explorer (Analogic)	CAS-One (CAScination AG)	Self-developed	Explorer (Analogic)	CAS-One (CAScination AG)	Explorer (Analogic)
Registration method	Sweep of anatomic landmarks on liver surface using tracked US probe and match with 3D model.	Phase 1: Common liver surface landmarks between 3D model and liver. Phase 2: Common liver surface and intraparenchymal landmarks between 3D model and liver. Phase 3: Sweep of liver using tracked US probe, automatic vasculature segmentation in 3D US volume, and automatic alignment to 3D model.	Common internal landmarks between 3D model and liver.	Sweep of anatomic landmarks on liver surface using tracked US probe and match with 3D model	Sweep of liver using tracked US probe, automatic vasculature segmentation in 3D US volume, and automatic alignment to 3D model.	Sweep of anatomic landmarks on liver surface using tracked US probe and match with 3D model
Visualization	1. Real-time US imaging. 2. Position and orientation of up to two tracked instruments relative to 3D virtual model. 3. Two crosshair views of preoperative CT.	1. Real-time US images with co-registered preoperative image data. 2. Position and orientation of tracked instrument relative to 3D virtual model. 3. 2D visualization of lateral and longitudinal displacement view relative to a selected target structure (e.g. a lesion).	1. Real-time US images with 3D model of tumor and needle trajectory overlayed. 2. Preoperative CT with real-time needle trajectory overlayed. 3. Position and orientation of up to two tracked instruments relative to 3D virtual model.	1. Real-time US imaging. 2. Position and orientation of up to two tracked instruments relative to 3D virtual model. 3. Two crosshair views of preoperative CT.	1. Real-time US images with co-registered preoperative image data. 2. Position and orientation of tracked instrument relative to 3D virtual model. 3. 2D visualization of lateral and longitudinal displacement view relative to a selected target structure	1. Real-time US imaging. 2. Position and orientation of up to two tracked instruments relative to 3D virtual model. 3. Two crosshair views of preoperative CT.
Outcomes	Initial experience using an image-guidance system with navigated US.	Suitable indications for navigation systems in open liver surgery and MWA.	Complete ablation rate of the first session, the local tumor progression (LTP), intrahepatic recurrence and disease-free survival.	Percentage of sonographically occult DLMs subsequently identified with image guidance	Benefits of going into computer assisted targeting techniques and microwave technology; pitfalls and overview of outcomes.	Percentage of sonographically occult DLMs subsequently identified with image guidance

2.3 Results

The application of navigation using 3D models during liver ablation with intraprocedural registration to US has been described in eight studies. Two of these articles are non-clinical studies (Table 2.1) and the other six articles report on clinical studies (Table 2.2). Navigation methods and results of the obtained articles will be covered in the following sections.

2.3.1 Instrument Tracking

Tracking of the instruments, amongst which the ablation needle, was performed either optically or electromagnetically. Optical tracking seems to be the most common in navigated ablations. Active optical tracking uses cameras to detect the 3D position and orientation of flashing light emitting diodes, which can be mounted on any surgical instrument. More common however is passive optical tracking, which relies on camera systems that emit near infrared (IR) light. Instruments which are required to be tracked are equipped with retro-reflective markers, which reflect the incoming light back to the cameras. The reflections are detected by the camera and then internally processed by the optical tracking system. These systems are wireless but the clinician has to deal with line-of-sight issues, as the tracking cameras require direct sight of the retro-reflective markers on the tracked tools [25].

This problem is overcome when using electromagnetic (EM) tracking systems, that consists of a field generator, control electronics and EM sensors. The field generator emits a magnetic field of a known geometry. Unique voltages are induced within the sensors, when these are placed in the EM field. These voltages are detected by a processor, which calculates the position and orientation of the sensors [26]. A drawback of EM tracking is its sensitivity to interference of large ferromagnetic objects nearby the field generator, distorting the magnetic field and affecting the accuracy [27,28].

The tip of the ablation needle is the part that transfers its energy to the tumor tissue. Tracking of the ablation needle is ideally performed by tracking the tip of the needle, as this theoretically accounts better for tip deflection or bending and result in more accurate needle positioning inside the tumor [29]. This is especially the case in laparoscopic and percutaneous ablation and to a lesser extent in open ablation, as in open ablation the needle is shorter and therefore less flexible. Also, in open ablation the clinician does not have to maneuver around structures such as the ribs before inserting the needle in the liver. Tip tracking is not possible for optical devices, as the sensor has to be visible to the IR camera, but can be integrated in EM tracking devices. Nevertheless, placement of an EM tracker in the tip of the needle arises other issues, such as the small volume available for the sensor and the localized energy coming from the tip, which can cause heating of and damage to the sensor. These difficulties have resulted in the fact that none of the articles included in this study have described tracking of the tip of the ablation needle.

2.3.2 Navigation Systems and Registration Methods

There are two FDA approved liver navigation systems. The Explorer Liver system (Analogic Inc., Boston, MA) was the first medical device to receive FDA clearance to navigate liver surgery using pre-operative images. However, the Explorer Liver system is currently no longer commercially available [24]. A similar system was developed by CAScination (Bern, Switzerland): the CAS-One system. Both systems have integrated tracking of ablation needles in their navigation software [30].

Accurate matching of the preoperative 3D model to the intraoperative position and orientation of the organ is crucial, especially in the case of performing ablations solely guided by the navigation system when lesions are not detected using conventional US. The process of registration can be challenging in liver surgery, as the liver is an organ that moves and deforms within the abdomen, particularly during open surgery in which liver tissue is palpated, lifted and dissected. There are multiple methods of registration.

Firstly, the Explorer system uses liver surface data acquired from a tracked probe. Pak et al. [24] used a probe to sweep four anatomic areas on the liver surface: the round and falciform ligament, and the left and right inferior borders of the liver. Subsequently, the system matched the location of these four areas with the 3D model. This method provides an accurate registration on the liver surface (2 to 6 mm in target surface areas) but not necessarily at the intraparenchymal structures [31]. This can be a problem for navigated ablations, as tumors located deeper in the parenchyma require an accurate registration to be targeted.

Secondly, the CAS-One system uses semi-automatically extracted vessel features for registration. During surgery, a 3D US volume is acquired in which vascular structures are automatically segmented in the individual slices and compounded to a 3D vessel structure. This US volume is then automatically aligned with the preoperative 3D model and accurate alignment is confirmed by the surgeon. Banz et al. [20] described a target registration error of 4.5 ± 3.6 mm.

2.3.3 Visualization Intraoperative Navigation

3D modelling of the liver based on preoperative images can be performed using software packages as Scout™ Liver (Analogic Inc., Boston, MA) or free navigation software amongst which 3D Slicer (3D Slicer contributors, https://www.slicer.org/). It is also possible to outsource modelling of the liver e.g. using MeVis Distant Service (MeVis Research, Bremen, Germany). Structures such as the liver, tumor(s), cysts and vasculature are visualized for guidance of the ablation. In the case of guiding percutaneous ablation, it can be useful to visualize the ribs. This way, the clinician can avoid vital structures and choose the most optimal needle trajectory.

The tracked instruments, such as the US and the ablation needle are modelled for visualization in the software. Real-time US images are displayed alongside the virtual model. The standard view of navigation software is the 3D visualization of the tool (e.g., US probe, ablation needle) position and orientation relative to the preoperative model, providing orientation to the surgeon. This is typically displayed on a touch screen covered by a sterile drape, allowing the surgical team to directly interact with the software.

Additional views can help facilitate interpretation by the surgeon. For example, the 2D visualization of lateral and longitudinal displacement relative to a selected target structure can be in an intuitive method to aid needle placement in 3D (Figure 2.2) [19, 20].
An alternative way to visualize this is by displaying the axial and sagittal orientation of preoperative CT showing the intraoperative position of the ablation needle (crosshairs) in addition to the 3D model and real-time US imaging [12].

A more extensive preoperative planning is possible by planning the optimal needle trajectory and ablation volume prior to the procedure and integrating this in the virtual navigation [21,23]. Tumor size is the most limiting factor in ablative therapy, as a lesion size greater than 3 cm is a significant predictor for decreased recurrence-free survival [32]. Large and irregular lesions require multiple ablations for complete tumor removal [21]. Visualization of multiple needle trajectories and ablation volumes can result in optimized needle placement to achieve a sufficiently large ablation zone and to maximize the remaining healthy liver tissue [33].

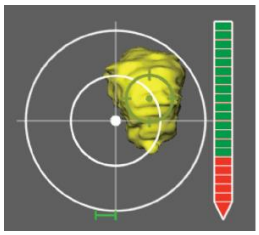

Figure 2.2: CAScination software; 2D visualization of lateral and longitudinal displacement relative to a selected target structure [20].

2.3.4 Post-procedure Evaluation

Non-clinical studies have shown the additional value of virtual navigation during ablation with a significant increase in puncture accuracy [18,19]. Moreover, the detection rate of tumors in a liver model is also significantly higher when using navigation. This improvement in performance is seen across all levels of training (residents, fellows and experience hepatobiliary surgeons) [19].

Clinical studies mainly focus on identifying suitable indications for the use of navigation systems in liver ablation and surgery. These studies show that navigation is particularly beneficial in cases where usefulness of conventional US is limited by complex anatomy, tumor location or echogenicity [12, 20,23]. Examples of indications for navigated ablation are multiple ablations of smaller tumors, poorly visible tumors using traditional guidance and parenchyma-sparing ablations.

Two studies have described the use of navigation in open liver ablation specifically for tumor(s) seen on preoperative imaging but undetectable on intraoperative US, i.e., disappearing liver metastases (DLMs) [22,24]. Kingham et al. [22] surveyed fourteen patients with 22 DLMs using navigation and subsequently identified fifteen (68%) of these tumors. This ratio is significantly lower in Pak et al. [24], in which 16% of the DLMs not detected using conventional US were located with image guidance. Both studies show navigation can aid surgeons in the identification of DLMs and facilitate the complete surgical clearance of all sites of liver disease.

At last, Zhang et al. [21] shows the complete percutaneous ablation rate of the first session to be higher when using 3D navigation than US-guidance only. With a mean follow-up period of 11.4 ± 4.9 months in the 3D group and 9.8 ± 5.5 months in the US group, there were no significant differences in te chnique efficacy rate and LTP rate between the two groups.

2.4 Recommendations Based on the Literature

- Instrument tracking can be done optically or electromagnetically. Tracking of the ablation needle is ideally done internally at the tip of the needle, as this could theoretically better account for tip deflection or bending and result in more accurate needle positioning inside the tumor [29]. However, this remains difficult to integrate.
- US volume registration is the most promising and accurate registration modality for registration of the preoperative model to intraprocedural US with an accuracy of 5 mm or less [20, 34].
- Navigated ablation improves puncture performance to conventional US in non-clinical studies [18,19].
- Navigation could be of additional value in the planning of multiple antenna placement [21].
- Navigation serves as a useful adjunct to aid in the identification of poorly visible (e.g., very small or vanishing) lesions on conventional US in open and percutaneous ablation [21, 24].
- Navigation is of particular importance in complex ablations, e.g., parenchyma-sparing treatments rather than for standard liver resections [19, 20].
- Navigation could be proven helpful as a training tool for ablation in residency [19].

2.5 Discussion

Hepatic tumor ablation has become a well-accepted tool in the treatment of both primary and metastatic lesions. The majority of hepatic ablation procedures are performed using ultrasound as guidance. Yet, this modality suffers from several shortcomings (e.g., low resolution, suboptimal orientation, tissue echogenicity) which limit its effectiveness in discriminating between tumor and healthy tissue. Navigation has proven to overcome some of these challenges.

Although navigation based on preoperative 3D modelling for liver ablation is increasingly used in clinical practice, there is limited prospective literature on this topic. Included articles were mostly small, retrospective non-randomized trials. Moreover, most of the clinical studies did not solely investigate navigated liver ablation but ablation during hepatic resections. In selected cases, outcomes were mainly focused on resection. Prospective, randomized controlled trials should be performed investigating clinically relevant endpoints (e.g. morbidity and mortality, complication rate, local tumor progression and overall survival) between conventional US guided and navigated ablations.

In addition, most articles describe navigated ablation specifically for use during open surgery. This is most likely because commercial liver navigation systems were initially developed for hepatic surgery. Nonetheless, navigation could be particularly helpful in laparoscopic hepatic surgeries and interventional treatments, due to the missing of haptic feedback and complexity of these procedures. An initial validation study of the Explorer Minimal Invasive Liver (MIL) was performed by comparing guidance information obtained from the system to intraoperative US. More specifically, the distance from the needle tip to the tumor was defined on US and on the Explorer system and these distances are compared. This study shows that the needle position on the Explorer MIL correlates strongly (5.5 ± 5.6 mm) with the probe position on intraoperative US [35]. Also, a comparable registration accuracy of the laparoscopic system to that provided in open IGS is shown [36]. However, in these studies, the Explorer MIL system was not used to assist in the placement of the probe. Clinical research studying navigated ablations in minimal invasive treatment modalities should follow.

Although not reported on within the scope of this review, it is possible to track the tip of the ablation needle. Accurate EM tip tracking (tracking error < 2 mm) has been described in a phantom, ex vivo and in vivo study by Kang et al. [37], in which the sensor is embedded in the small space of the cooling system of RF antenna. Embedding the sensor in this specific location may affect the ablation performance due to the decreased flow of circulating chilled water. This study showed no significant difference of total delivered energy and impedance between the conventional probe and the one with the embedded EM sensor. Furthermore, Sindram et al. [38] evaluated a commercially available EM tip tracking device (AIM™ Guidance System; InnerOptic Technology, Inc., Hillsborough, NC, USA) for laparoscopic MWA of liver tumors in thirteen patients. The success rate of first-attempt needle placements was 93%. Nevertheless, these ablation needles, including the embedded sensors, are disposables therefore the cost-effectiveness is yet to be determined as generally sensors used for tracking of the shaft can be re-used.

The most important limitation of the included studies is the inability to continuously register the preoperative model to the liver. Once the liver is moved or deformed e.g. due to surgical manipulation, re-registration is required or else accuracy is lost. Ideally, the navigation system allows for constant updates of the registration.
The challenge of liver movement also arises due to patient respiration, which can displace the liver with up to 30 mm in craniocaudal direction with each breath, decreasing the accuracy of the navigation [23]. Typical ways to tackle this problem include breath hold, respiratory gating and tracking, and active breathing control [39]. When considering the articles included in this research, compensating for liver motion due to patient respiration has only been described by Beerman et al. [23]. They performed active breathing control by high-frequency jet ventilation (HFJV). HFJV is a ventilation technique in which gas of sub-dead space tidal volumes is delivered in a high frequency, which minimizes lung movement. Therefore abdominal organ movement is also minimized to 2-3 mm [40].

Future work on navigated liver ablation should focus on compensation for organ motion and deformation.

References

1. Gallinger, S., Biagi, J. J., Fletcher, G. G., Nhan, C., Ruo, L., & McLeod, R. S. (2013). Liver resection for colorectal cancer metastases. Current Oncology, 20(3), e255.
2. Gena P Kanas, Aliki Taylor, John N Primrose, Wendy J Langeberg, Michael A Kelsh, Fionna S Mowat, Dominik D Alexander, Michael A Choti, and Graeme Poston. Survival after liver resection in metastatic colorectal cancer: review and meta-analysis of prognostic factors. Clinical epidemiology, 4:283, 2012.
3. PC Simmonds et al. "Surgical resection of hepatic metastases from colorectal cancer: a systematic review of published studies". In: British journal of cancer 94.7 (2006), p. 982.
4. Glassberg, M. B., Ghosh, S., Clymer, J. W., Wright, G. W., Ferko, N., & Amaral, J. F. (2019). Microwave ablation compared with hepatic resection for the treatment of hepatocellular carcinoma and liver metastases: a systematic review and meta-analysis. World journal of surgical oncology, 17(1), 98.
5. Takahashi, H., & Berber, E. (2020). Role of thermal ablation in the management of colorectal liver metastasis. Hepatobiliary Surgery and Nutrition, 9(1), 49.
6. Wells, S. A., Hinshaw, J. L., Lubner, M. G., Ziemlewicz, T. J., Brace, C. L., & Lee, F. T. (2015). Liver ablation: best practice. Radiologic Clinics, 53(5), 933-971.
7. Citone, M., Fanelli, F., Falcone, G., Mondaini, F., Cozzi, D., & Miele, V. (2020). A closer look to the new frontier of artificial intelligence in the percutaneous treatment of primary lesions of the liver. Medical Oncology, 37, 1-7.
8. Bao, P., Sinha, T. K., Chen, C. C., Warmath, J. R., Galloway, R. L., & Herline, A. J. (2007). A prototype ultrasound-guided laparoscopic radiofrequency ablation system. Surgical endoscopy, 21(1), 74-79.
9. Peterhans, M., vom Berg, A., Dagon, B., Inderbitzin, D., Baur, C., Candinas, D., & Weber, S. (2011). A navigation system for open liver surgery: design, workflow and first clinical applications. The international journal of medical robotics and computer assisted surgery, 7(1), 7-16.
10. Seror, O. (2014). Percutaneous hepatic ablation: what needs to be known in 2014. Diagnostic and interventional imaging, 95(7-8), 665-675.
11. Joo, I. (2015). The role of intraoperative ultrasonography in the diagnosis and management of focal hepatic lesions. Ultrasonography, 34(4), 246.
12. Kingham, T. P., Scherer, M. A., Neese, B. W., Clements, L. W., Stefansic, J. D., & Jarnagin, W. R. (2012). Image-guided liver surgery: intraoperative projection of computed tomography images utilizing tracked ultrasound. HPB, 14(9), 594-603.
13. Kruskal, J. B., & Kane, R. A. (2006). Intraoperative US of the liver: techniques and clinical applications. Radiographics, 26(4), 1067-1084.
14. Perrodin, S., Lachenmayer, A., Maurer, M., Kim-Fuchs, C., Candinas, D., & Banz, V. (2019). Percutaneous stereotactic image-guided microwave ablation for malignant liver lesions. Scientific reports, 9(1), 1-8.
15. Kuhlmann, K., Van Hilst, J., Fisher, S., & Poston, G. (2016). Management of disappearing colorectal liver metastases. European Journal of Surgical Oncology (EJSO), 42(12), 1798-1805.
16. Stone, M. J., & Wood, B. J. (2006, March). Emerging local ablation techniques. In Seminars in interventional radiology (Vol. 23, No. 1, p. 85). Thieme Medical Publishers.
17. Moher, D., Liberati, A., Tetzlaff, J., & Altman, D. G. (2010). Preferred reporting items for systematic reviews and meta-analyses: the PRISMA statement. Int J Surg, 8(5), 336-341.
18. Wu, W., Xue, Y., Wang, D., Li, X., Xue, J., Duan, S., & Wang, F. (2015). Application of 3D imaging in the real-time US–CT fusion navigation for minimal invasive tumor therapy. International journal of computer assisted radiology and surgery, 10(10), 1651-1658.

19. Martin, R. C., & North, D. A. (2016). Enhanced ultrasound with navigation leads to improved liver lesion identification and needle placement. Journal of Surgical Research, 200(2), 420-426.
20. Banz, V. M., Müller, P. C., Tinguely, P., Inderbitzin, D., Ribes, D., Peterhans, M., ... & Weber, S. (2016). Intraoperative image-guided navigation system: development and applicability in 65 patients undergoing liver surgery. Langenbeck's archives of surgery, 401(4), 495-502.
21. Zhang, D., Liang, W., Zhang, M., Liang, P., Gu, Y., Kuang, M., ... & Yu, J. (2018). Multiple antenna placement in microwave ablation assisted by a three-dimensional fusion image navigation system for hepatocellular carcinoma. International Journal of Hyperthermia, 35(1), 122-132.
22. Kingham, T. P., Pak, L. M., Simpson, A. L., Leung, U., Doussot, A., D'Angelica, M. I., ... & Jarnagin, W. R. (2018). 3D image guidance assisted identification of colorectal cancer liver metastases not seen on intraoperative ultrasound: results from a prospective trial. HPB, 20(3), 260-267.
23. Beermann, M., Lindeberg, J., Engstrand, J., Galmén, K., Karlgren, S., Stillström, D., ... & Freedman, J. (2019). 1000 consecutive ablation sessions in the era of computer assisted image guidance–lessons learned. European journal of radiology open, 6, 1-8.
24. Pak, L. M., Gagnière, J., Allen, P. J., Balachandran, V. P., D'Angelica, M. I., DeMatteo, R. P., ... & Kingham, T. P. (2019). Utility of image guidance in the localization of disappearing colorectal liver metastases. Journal of Gastrointestinal Surgery, 23(4), 760-767.
25. Poulin F, Amiot LP. Interference during the use of an electromagnetic tracking system under OR conditions. J Biomechanics. 2002;35(6):733–737.
26. Lange, T., Hünerbein, M., Eulenstein, S., Beller, S., & Schlag, P. M. (2006). Development of navigation systems for image-guided laparoscopic tumor resections in liver surgery. In Minimally Invasive Tumor Therapies (pp. 13-36). Springer, Berlin, Heidelberg.
27. Sindram, D., McKillop, I. H., Martinie, J. B., & Iannitti, D. A. (2010). Novel 3-D laparoscopic magnetic ultrasound image guidance for lesion targeting. Hpb, 12(10), 709-716.
28. Sadjadi H, Hashtrudi-Zaad K, Fichtinger G. Simultaneous electromagnetic tracking and calibration for dynamic field distortion compensation. IEEE Trans Biomed Eng. 2016;63(8):1771–1781.
29. Wood, B. J., Kruecker, J., Abi-Jaoudeh, N., Locklin, J. K., Levy, E., Xu, S., ... & Venkatesan, A. M. (2010). Navigation systems for ablation. Journal of Vascular and Interventional Radiology, 21(8), S257-S263.
30. Simpson, A. L., & Kingham, T. P. (2016). Current evidence in image-guided liver surgery. Journal of Gastrointestinal Surgery, 20(6), 1265-1269.
31. Cash, D. M., Miga, M. I., Glasgow, S. C., Dawant, B. M., Clements, L. W., Cao, Z., ... & Chapman, W. C. (2007). Concepts and preliminary data toward the realization of image-guided liver surgery. Journal of Gastrointestinal Surgery, 11(7), 844-859.
32. Meloni, M. F., Chiang, J., Laeseke, P. F., Dietrich, C. F., Sannino, A., Solbiati, M., ... & Lee Jr, F. T. (2017). Microwave ablation in primary and secondary liver tumors: technical and clinical approaches. International Journal of Hyperthermia, 33(1), 15-24.
33. Bale, R., Widmann, G., & Jaschke, W. (2011). Navigated open, laparoscopic, and percutaneous liver surgery. Minerva chirurgica, 66(5), 435.
34. Ribes, D., Peterhans, M., Anderegg, S., Wallach, D., Banz, V., Kim-Fuchs, C., ... & Weber, S. (2012). Towards higher precision in instrument guided liver surgery: automatic registration of 3D ultrasound with pre-operative MeVis-CT. Int J Comput Assist Radiol Surg, 7(Suppl 1), S141-S142.
35. Hammill, C. W., Clements, L. W., Stefansic, J. D., Wolf, R. F., Hansen, P. D., & Gerber, D. A. (2014). Evaluation of a minimally invasive image-guided surgery system for hepatic ablation procedures. Surgical innovation, 21(4), 419-426.

36. Kingham TP, Jayaraman S, Clements LW, Scherer MA, Stefansic JD, Jarnagin WR (2013) Evolution of image-guided liver surgery: transition from open to laparoscopic procedures. J Gastrointest Surg 17:1274–1282
37. Kang, T. W., Lee, M. W., Choi, S. H., Rhim, H., Lim, S., Song, K. D., ... & Yang, J. (2015). A novel electrode with electromagnetic tip tracking in ultrasonography-guided radiofrequency ablation: a phantom, ex vivo, and in vivo experimental study. Investigative radiology, 50(2), 81-87.
38. Sindram, D., Simo, K. A., Swan, R. Z., Razzaque, S., Niemeyer, D. J., Seshadri, R. M., ... & Martinie, J. B. (2015). Laparoscopic microwave ablation of human liver tumors using a novel three-dimensional magnetic guidance system. HPB, 17(1), 87-93.
39. Salati, U., Barry, A., Chou, F. Y., Ma, R., & Liu, D. M. (2017). State of the ablation nation: a review of ablative therapies for cure in the treatment of hepatocellular carcinoma. *Future Oncology*, 13(16), 1437-1448.
40. Galmén, K., Harbut, P., Freedman, J., & Jakobsson, J. G. (2017). The use of high-frequency ventilation during general anaesthesia: an update. F1000Research, 6.

Chapter 3

Tracking of the ablation needle

The first goal of this thesis was to develop a method to track the position and orientation of the microwave ablation needle using electromagnetic tracking. An adapter was created containing the EM sensor which can be attached to the ablation needle. A pivot calibration of the adapter was performed. Subsequently, the adapter was validated for usability, sterilizability and reproducibility of the calibration and tracking accuracy.

3.1 Introduction

The microwave antenna used at our institute is the 15 cm Emprint™ percutaneous microwave antenna (Medtronic, Minneapolis, MN). Medtronic also has Emprint™ SX navigation antennas, but these antennas are only compatible with the Emprint SX electromagnetic field generator, which is not available in Europe. Hence, another tracking method should be explored. It is of importance to investigate the different options of tracking to use the most suitable method in the current workflow.

Literature on EM navigated liver ablation explore either tracking a needle guide or the needle itself. In case of a guided approach, the needle is inserted through a tracked applicator, usually connected to the intra-operative US [1,2]. Here, the US probe is tracked electromagnetically and the needle trajectory is virtually overlaid in the US image and 3D model (Figure 3.1). As the ablation needle is also tracked, the depth of the needle insertion can be overlaid. An applicator for the ablation probe connected to the US can be useful as it shows the needle trajectory automatically in the center of the US image, and when the desired needle trajectory is determined, the surgeon does not have to determine the depth of the needle insertion. However, since the guide is rigidly attached to the US, it might limit the surgeon's freedom in adjusting the needle insertion. When tumor and critical structures are optimally displayed on the US, this does not necessarily result in the optimal needle trajectory for ablation.
Paolucci et al. [3] have developed an EM tracked needle guide for laparoscopic navigated liver ablations (Figure 3.2). An advantage of this method is that the guide prevents needle deflection. However, there are several shortcomings to this method.
First, since the trocar diameter is larger than the needle, it requires a larger incision. Secondly, when the trocar is not directly positioned perfectly into the tumor and therefore repositioned, tumor cells could spread into the healthy surrounding tissue. This risk is also present when no trocar is used and the ablation needle is repositioned for optimal placement into the tumor, but then the risk of tumor spread is overcome by continuing the ablation while pulling the needle back. Also, directly navigating the ablation needle could be favorable, as this limits changes to the current surgical workflow at the NKI-AvL during open liver ablation.

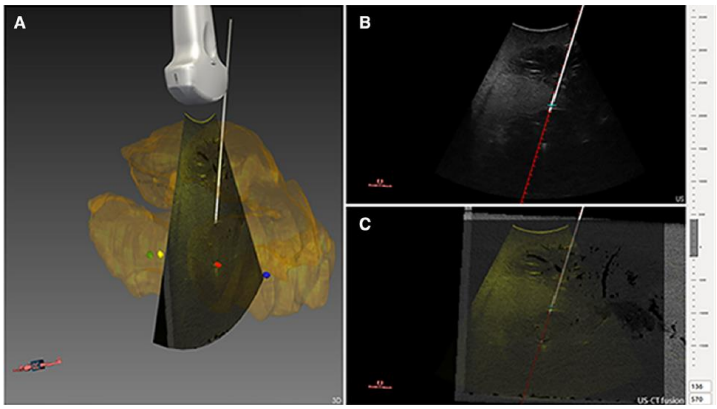

Figure 3.1: Guided needle insertion through US applicator [1].

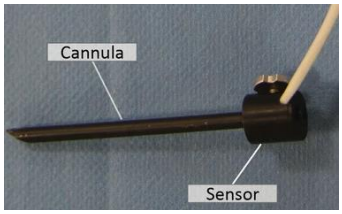

Figure 3.2: EM tracked trocar for insertion of the ablation probe as described by Paulucci et al [3].

More often mentioned in literature than the guided approach is the freehanded approach. During this approach, the surgeon places the ablation needle freely on the liver surface. In these approaches the needle itself is tracked.
Electromagnetically, the ablation needle can be tracked either at its tip or it shaft. The tip is the part of the needle that transfers its energy to the tumor tissue. Tracking at the tip is ideal as deflection or bending of the needle will not affect the tip position, thus resulting in a more accurate tracking/navigation [4]. Only one system which implements tip tracking is described in literature; the eTRAX™ Needle Tip Tracking System by CIVCO Medical Solutions (Coralville, IA, USA). The eTRAX™ is a needle-like device that contains an EM sensor, which can be placed inside a special biopsy or ablation needle. The sensor is first placed in a sterile cover (Figure 3.3a), which is then inserted into an ablation needle (Figure 3.3b). At last, the handle of the sensor is locked onto the handle of the needle (Figure 3.3c). A study shows successful percutaneous RFA of four liver lesions performed in three patients using the eTRAX™ system [6]. Nevertheless, the eTRAX™ system is only available for RFA needles and not for MWA needles, which are used for open ablation at the NKI-AvL.

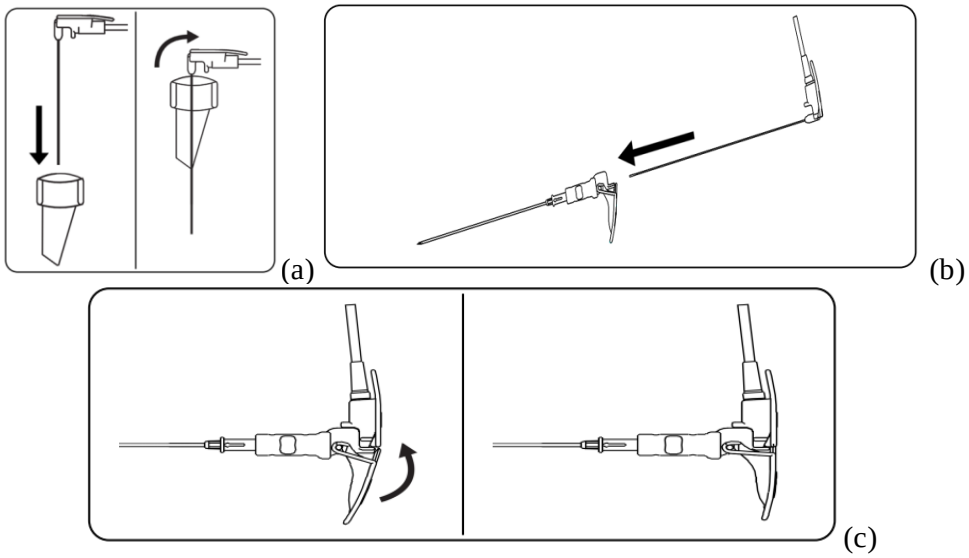

Figure 3.3: eTRAX Needle Tip Tracking System by CIVCO Medical Solutions [5].

Even though tip tracking can be favorable in laparoscopic and percutaneous ablations, this is of less importance in open ablations. This is because in open ablation the clinician does not have to guide the needle across anatomical structures such as the ribs to reach the liver. Also, the needle used for open ablations is shorter and therefore more rigid. A recent study that investigated ablation needle deflection after placement of the antenna into the tumor, showed that maximal needle deflection tends to increase with insertion depth (Figure 3.4) [7]. In this study, ablation needles deflected 1.3 mm on average during percutaneous liver ablation. The needles investigated in this study were either 14 or 17 Gauges in diameter. As the insertion depth of the antenna during open ablation is limited and the Emprint antennas used in the NKI-AvL have a larger diameter (11 Gauges) than those used in the aforementioned study, we assumed that needle deflection will play a minimal role during open liver ablation. However, it should be noted that this study explored needle deflection after placement in the tumor, while during placement it is possible that needle deflection is larger.

While tip tracking might overcome the problems of bending, it is difficult to implement. Firstly, placement of an EM tracker in the tip of the needle might cause malfunction of the sensor due to the heating at the tip. Secondly, this would require a safety validation of new ablation needle (i.e. CE marking). Due to existing challenges and expected minimal benefit of tip tracking compared to shaft tracking, it is chosen to track the shaft of the ablation needle.

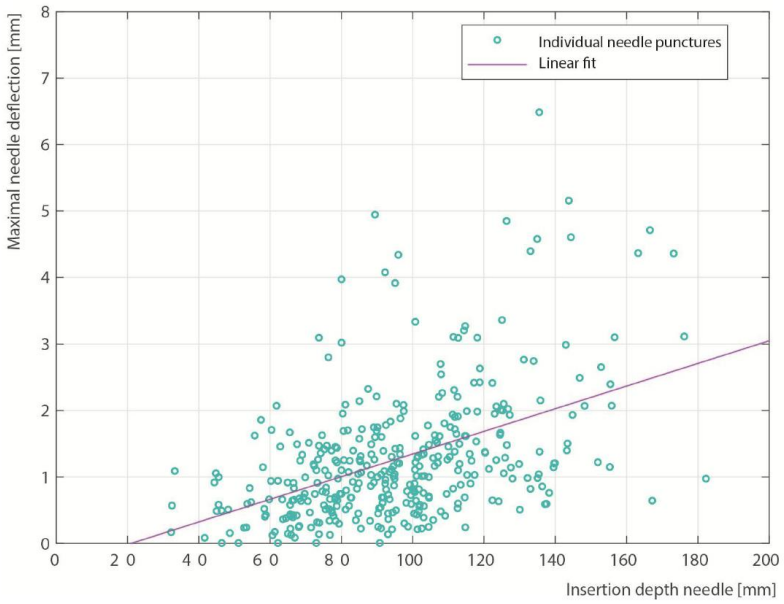

Figure 3.4: Scatterplot of the maximal needle deflection of 365 needle insertions during percutaneous thermal ablation procedures of liver tumors [7].

For shaft tracking, an adapter was created to connect the EM sensor to the shaft of the MWA probe. 3D printing offers the advantages of creating an adapter compatible with the percutaneous microwave antenna (Medtronic, Minneapolis, MN) (Figure 3.5a) used at the NKI-AvL, as well as the EM sensors currently used for the surgical navigation, the Aurora 6DOF cable tools ⌀2.5mm × 2m length (NDI, Waterloo, ON) (Figure 3.5b). These EM sensors have a high tracking accuracy, as shown in Table 3.1 [8].

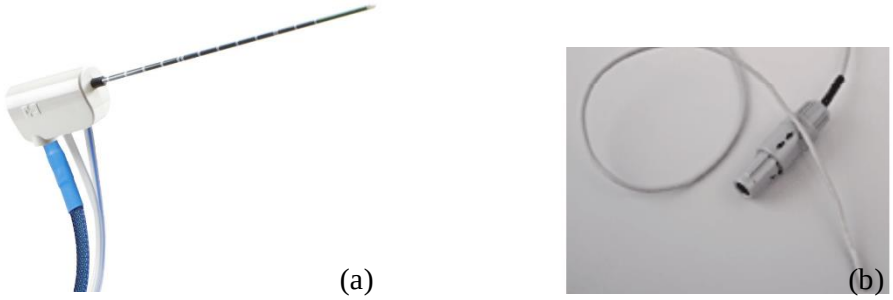

(a) (b)

Figure 3.5: (a) The Emprint™ microwave ablation needle and (b) the Aurora 6DOF electromagnetic sensor.

Table 3.1: The Root Mean Squared Errors of the Aurora 6DOF Sensor in combination with the field generator [8].

	Cube volume FG	*Dome volume FG*
Position	0.48 mm	0.70 mm
Orientation	0.30°	0.30°

3.2 Methods

3.2.1 Adapter Design and Printing

Before designing the adapter, a list of requirements was developed in consultation with the hepatobiliary surgeons of the NKI-AvL and involved researchers (Table 3.2). It was chosen to glue the sensor inside an opening in the adapter, which should completely fill the remaining space in the opening for the sensor. Therefore, there is no possibility for bacteria and micro-organisms to enter, which would be difficult to sterilize.

Table 3.2: List of Requirements adapter for the EM tracking of an ablation needle.

Usability	Adapter position does not hinder the conventional handling/use of the ablation needle.
	Does not have sharp edges that can potentially rupture gloves or sterile covers.
	Mounting onto ablation probe takes less than one minute with minimal training.
	Easy to attach and detach without damaging adapter, sensor or probe.
Materials	Do not influence EM field (non-ferromagnetic).
	Should not break during attachment and detachment.
	Sterilizable (can withstand autoclave or STERRAD cycle).
	Adapter is preferably printable with the Formlabs Form 3B 3D printer.
	Glue is suitable for the printing material as well as the silicon of the Aurora cable tool.
Result	Connects Aurora 6DOF EM sensor ⌀2.5mm (NDI, Waterloo, ON) to the short Emprint™ percutaneous microwave antenna (Medtronic, Minneapolis, MN).
	No movement between sensor and adapter to ensure an accurate calibration.
	No movement between ablation needle and adapter after attachment to ensure an accurate calibration.
Other	Design does not contain any lumen apart from the opening for the sensor. The glue should completely fill the remaining space in the opening for the sensor.

A 3D optical scan of the ablation needle was made using an intra-oral optical scanner (TRIOS 3 Basic, 3Shape). This optical scan results in a Surface Tessellation Language (STL) file of the ablation needle, a file format that describes the surface geometry of a 3D. This scanner stitches several scans together using landmarks on the surface of the object to be scanned, thus resulting in a 3D model of it. Consequently, the adapter could be designed based on the obtained STL model to fit the exact shape of the ablation needle. The adapter was modelled in Meshmixer and Solidworks 2020 (Dassault Systèmes, Educational Edition, https://www.solidworks.com/).

The final design was 3D printed using the Formlabs Form 3B 3D printer available at the NKI-AvL. This is a Stereolithography (SLA) printer. SLA is an additive manufacturing process that uses a laser to harden a photopolymer resin. The ultraviolet (UV) laser draws the shape of the first layer of the 3D model that was uploaded to the printer. Photopolymers are solidified when exposed to UV light. The cured layer then separates from the tank containing the resin and a new layer is formed. This process is repeated until the print is completed.

The initial material evaluated was the Dental Model Resin by Formlabs. This resin was used in other research at the Head and Neck department at the NKI-AvL and can be printed with a high resolution (25 microns). This material resulted inappropriate for the adapter since, after ten runs of sterilization and attaching the adapters over a hundred times, one of the adapters broke. The Dental Model Resin is

a stiff material and attaching and detaching the adapters repeatedly resulted in material fatigue and breakage.

When performing a tensile test on a material, each material has an elastic region where the original dimensions of the material will be completely recovered when the applied load is removed. For larger stresses in the plastic region, permanent deformation will remain after the applied load is removed. The Young's Modulus is a measure of how stiff a material is. The higher the Young's modulus, the stiffer a material and so the smaller the elastic deformations will be for a given applied load. Another material property is the tensile strength, which indicates the maximum stress that a material can withstand before breaking. The BioMed Clear Resin by Formlabs has a slightly lower Young's Modulus and a higher tensile strength than the Dental Model resin. Hence, the adapters were printed in the Elisabeth-TweeSteden Hospital (ETZ) in Tilburg using the BioMed Clear Resin, as this was not directly available in our institute. The material can also be purchased at the NKI-AvL as it is compatible with the Form 3B 3D printer. This resulted in prints that did not break after attachment of the adapter for over a hundred times. Both materials are non-ferromagnetic and therefore do not influence the accuracy of the needle tracking.

The manufacturing process of the adapters was as follows. Three different adapters were printed with number one to three engraved at the back of the adapter, so they could be differentiated from each other. After the printing was finished, the adapters were removed from the build plate and washed in the Form Wash in 99% Isopropyl Alcohol (IPA) for 15 minutes to remove the uncured resin. The parts were removed from the IPA and left to air dry at room temperature for 30 minutes. When no residual alcohol or excess liquid resin remained on the surface, the parts were placed in the Form Cure at 60 °C for 60 minutes to achieve optimal material properties. Finally, support structures were removed and the adapters were then disinfected in fresh 99% IPA for 5 minutes. Elastosil silicon glue E41 (Wacker Chemie AG, München, Germany) was then used to glue the sensor in the adapter.

Approval for the design of the adapter and the Dental Model Resin was obtained by the Central Sterilization Department (CSD) of the NKI-AvL. We are currently expecting/waiting the approval for the BioMed Clear Resin by the CSD. The sterilization method, gas plasma sterilization using the STERRAD system (Advanced Sterilization Products (ASP), CA, USA), utilizes hydrogen-peroxide and low temperature gas plasma (an ionized gas) to sterilize materials. The radiofrequency plasma breaks apart the hydrogen-peroxide and a plasma cloud results. This cloud consists of UV light and free radicals, the combination of which kills all remaining bacteria and thus sterilizing the instrument. Consequently, the radiofrequency is turned off and the activated components lose their energy and recombine to form oxygen, water and non-toxic byproducts.
The advantage of this sterilization method is that the adapters can be sterilized within our institute, which in practice means they can be sterilized within a few hours. Also, the STERRAD does not use high temperatures, steam or pressure, which can potentially damage the sensor within the adapter.

3.2.2 Calibration

Calibration of the adapter was necessary to determine the needle position and orientation with respect to the sensor. Since the EM sensor are glued within the adapters, each adapter has its own calibration, as the sensor orientation within the adapter differs.
Calibration of the adapters was performed using a pivot calibration, which is a function of the NDI Track software. In this specific type of calibration, the transformation between the sensor and the tip of a tool is determined. First, the adapter was connected to the ablation needle. Then, the process consisted in pivoting the instrument around a conical shape on a stationary point with an angle ranging from 30 to 60 degrees. This pivoting was performed for 30 seconds with a frame frequency of 40 Hz. This results in a set of transformations $[R_i, t_i]_{i=1..m}$, which are all located on the surface of a sphere with the tip of the tool as the origin (Figure 3.6). NDI Track performed the sphere fitting and estimated the pivot point.

When the location of the tip was known, the tip offset between the EM sensor and the tip of the needle could be calculated [9].
The part of the Emprint™ ablation needle distributing the microwaves onto the tissue is marked green on the antenna. As we want our calibration to be at the center of the ablation zone, the size of the marked area on the antenna was measured using a caliper. Half of the ablation zone and the tip of the ablation needle was then cut off. Pivoting was performed on the remaining part of the ablation needle.

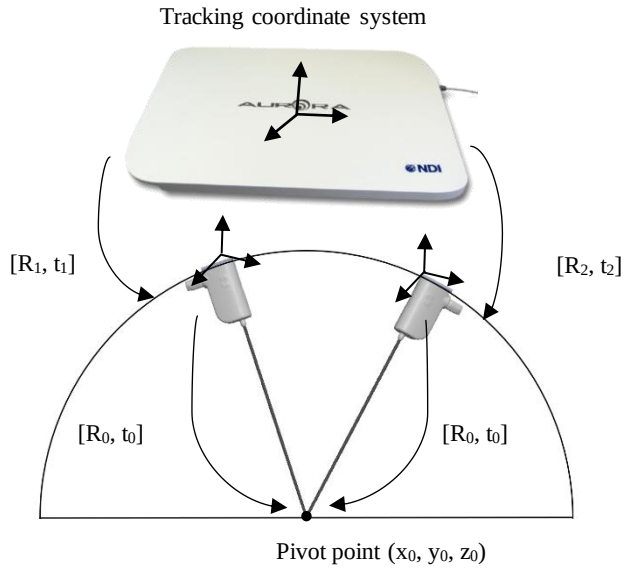

Figure 3.6: Pivoting calibration of ablation needle with sensor located at the back of its shaft, modified from [9].

3.2.3 Adapter Validation

Reproducibility Attachment Process on a Single Needle
To be able to use the same calibration matrix for one adapter without recalibrating the adapter every time is reattached to the ablation needle, it is important to confirm that the adapter will consistently attach to the adapter exactly at the same position each time. To validate this, a sensor was attached onto the shaft of the ablation needle as a reference (Figure 3.7). When the transformation from this reference sensor and the sensor within the adapter is the same each time the adapter is reattached, it can be concluded that the adapter does not need to be recalibrated each time after reattachment. The steps of this reproducibility test were as follows:

1. The adapter was mounted onto the ablation needle and the needle was placed in the center of the electromagnetic field.
2. The position and orientation of both sensors were then recorded for five seconds.
3. The adapter was detached.

These steps were repeated for twenty times. The position and orientation of the sensors during the recording of five seconds are averaged to account for jitter errors. Of the twenty samples, Euclidean distances and the three Euler angles (R_x, R_y, R_z) between the two sensors were calculated. The Euclidean distance between a point $p1(x,y,z)$ and point $p2(x,y,z)$ can be calculated using Formula 3.1. Consequently, the standard deviations (SD) of the twenty Euclidean distances and Euler angles were calculated to determine the variation.

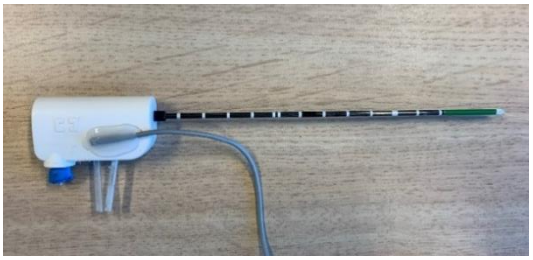

Figure 3.7: Sensor attached onto shaft of the ablation needle.

$$d(p1, p2) = \sqrt{((x_1 - x_2)^2 + (y_1 - y_2)^2 (z_1 - z_2)^2)} \quad (3.1)$$

Sterilization validation
After approval by the CSD was obtained for the design and materials, it was necessary to ensure that the sensor and adapter could withstand the cleaning and sterilization process. Thus, the adapter was sterilized in the STERRAD by the CSD ten times, as is standard in our institute. After sterilization, the accuracy of the calibration was checked using the method mentioned below in order to ensure that the calibration of the adapters was still valid.
For the adapter printed with the BioMed Clear Resin, the reproducibility of the attachment process was performed twenty times before and twenty times after sterilization to check whether the adapter did not undergo any surface changes and the process of attachment was still consistent.

Accuracy calibration
The accuracy of the calibration is determined and compared to that of the Aurora 6DOF surgical pointer by NDI (Northern Digital Inc. (NDI), Waterloo, Ontario, Canada) (Figure 1.7a). This surgical instrument, containing two 5DOF sensors holds a submillimeter accuracy within 32 cm distance of the field generator [10].
The tabletop field generator was connected and a tracked 3D printed block with eight small divots indicated with a number (Figure 3.8) was placed in the EM field. To determine the location and orientation of the block, eight landmarks were defined for registration. The surgical pointer was used to indicate the location of the eight points, which were then matched to the points in the software.
After registering the block, a distance measure from the tip of the pointer was set to each of the eight divots in the navigation software. Consequently, a person placed the pointer onto the eight divots without any information of the navigation software provided (Figure 3.8a). When the pointer was placed on the divot, a screenshot was made that indicates the distance from the tip of the pointer to the calibrated divots (Figure 3.8b). After performing this test with the pointer, it was executed with one ablation needle using two adapters of the Dental Model Resin and with three ablation needles using two adapters of the BioMed Clear Resin. This was due to the fact that at the time of the tests using the Dental Model Resin adapter, only one ablation needle was available for research.

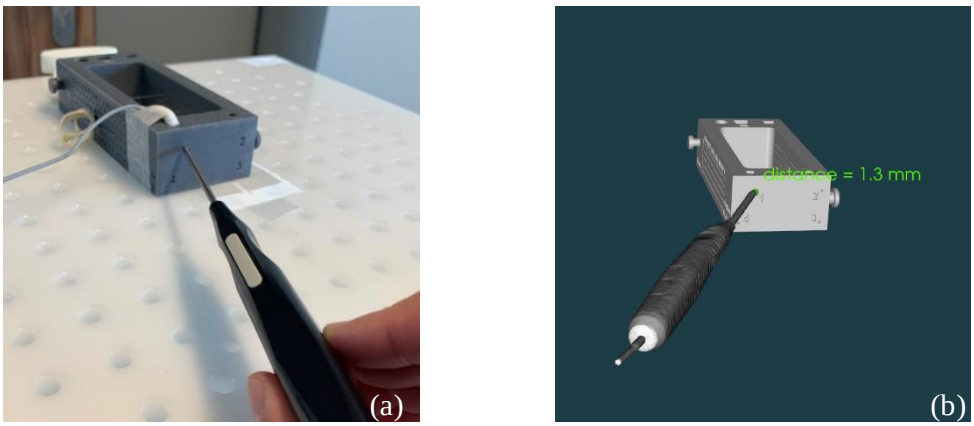

Figure 3.8: Testing the accuracy of the calibration and registration. Tests are performed using a tracked pointer and tracked ablation needle.

3.3 Results

3.3.1 Adapter Design

The final design of the adapter is shown in Figure 3.9. It is a simple clip-on system that carries the sensor at the back of the adapter (Figure 3.10). Due to its smooth finish with the surface of the ablation probe, it is not of inconvenience to the surgeon during the process of ablation. After a short instruction, a surgical nurse and a surgeon were able to attach the adapter to the ablation needle under sterile conditions without any difficulties. Attachment of the adapter is performed in less than ten seconds.

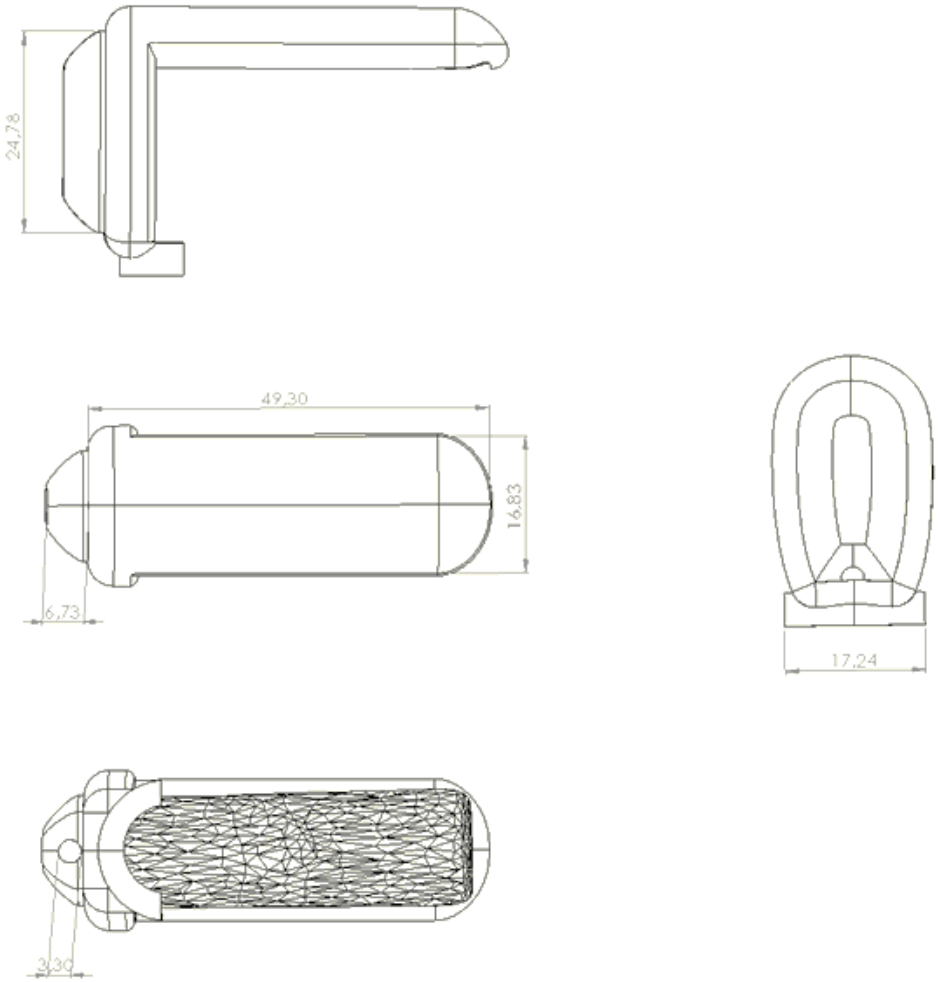

Figure 3.9: Technical drawings of adapter, dimensions in milimeters.

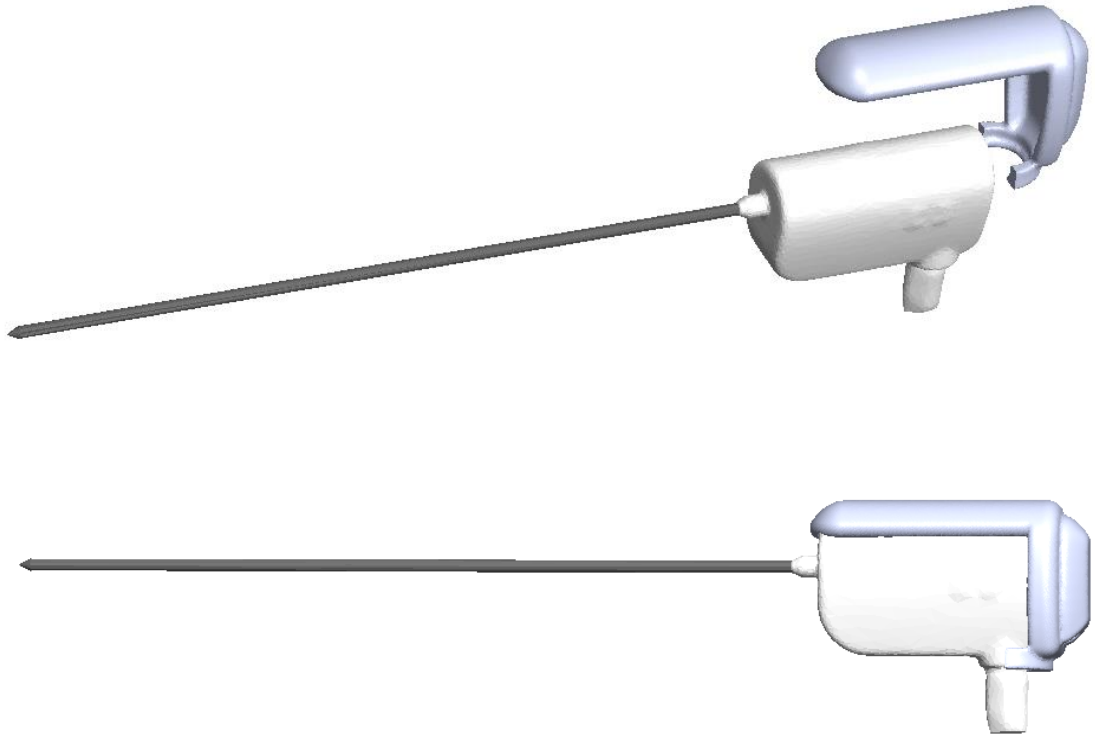

Figure 3.10: Attachment of the adapter to the Emprint ablation needle.

3.3.2 Adapter Validation

Reproducibility Attachment Process on a Single Needle and Material Sterilization
The adapter of both the Dental Model Resin and the BioMed Resin were attached to and detached from the ablation needle twenty times. After ten cycles of sterilization the reproducibility tests with the BioMed adapter were repeated. The standard deviations over these performed tests are shown in Table 3.3. The inaccuracies of both adapters are within the tracking accuracy of the sensor (Table 3.1). Therefore, it can be concluded that the location and orientation of the adapter is similar each time after attachment. Also, sterilization does not result in any surface changes of the BioMed adapter.

Table 3.3: Standard deviations of Euclidean distance and Euler angle between adapter and reference sensor after repeatedly reattaching the adapter.

	SD Euclidean Distance (mm)	SD R_x (°)	SD R_y (°)	SD R_z (°)
Dental Model adapter	0.04	0.03	0.23	0.2
BioMed adapter before sterilization	0.05	0.21	0.27	0.45
BioMed adapter before and after sterilization	0.08	0.18	0.36	0.44

Accuracy Calibration and Material Sterilization
The printed adapters could be sterilized repeatedly without any problems. The accuracies of the pointer and four different adapters of indicating the divots on the calibrated block are visualized in the boxplots in Figure 3.11. The Dental Model adapters were tested on one ablation needle and the BioMed adapters with three different ablation needles of which the results are averaged. On average, the pointer could indicate the eight divots with an accuracy of 2.3 mm. This error can arise from multiple sources, such as inaccuracies of the tracking, the challenge of indicating precisely at the divots and of the registration

error. The large registration error (RMSE> 1.0 mm), is most likely due to the fact that the calibration block has been printed with a material that has been slightly deformed over time.
The Dental Model Resin adapters demonstrated an accuracy of 2.6 and 1.7 mm and the BioMed adapters of 2.14 and 2.11 mm, which are comparable with the accuracy of the surgical pointer.
Nonetheless, as shown in Figure 3.11, the distance from the ablation needle to the divots could increase up to 4 mm. This could be the result of movement of the needle when the accuracy is being measured or the fact that the needle bends on the rigid surface of the calibration block.

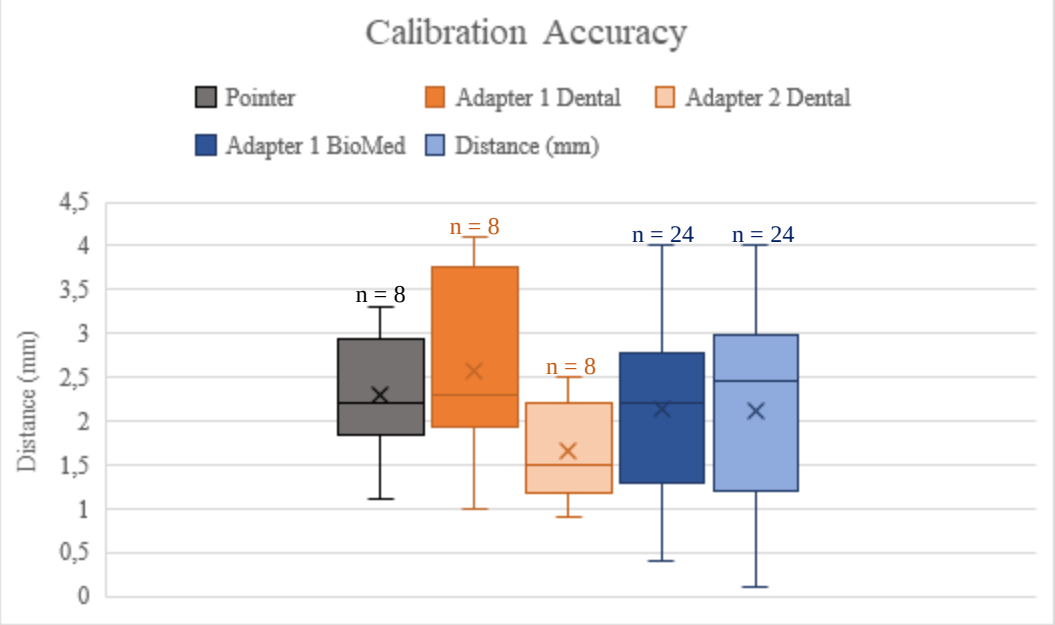

Figure 3.11: Accuracy of the pointer and adapters attached to ablation needles with respect to eight points a calibrated block. Tests were performed for one pointer, one ablation needle using two adapters of the Dental Model Resin and for three ablation needles using two adapters of the BioMed Clear Resin. Boxplots shows the median, quartiles and the cross indicates the mean.

3.4 Discussion

An adapter was created to track the Emprint™ MWA ablation needle. The adapter is sterilizable and can be easily attached to the ablation needle under sterile conditions by the surgeon. The calibration accuracy and reproducibility of the adapters showed satisfactory results.

Even though pivot calibration showed good results for the calibration of the adapter, it should be noted that there are multiple ways of calibration, each with its advantages and disadvantages. In this study, it was chosen to perform a pivot calibration as it is fast, accurate and no additional calibration devices are necessary. Nonetheless, it also has some limitations. A disadvantage of this calibration is that it cannot be performed during surgery, as the center of the ablation zone can only be defined after removal of a part of the antenna. In addition, a pivot calibration only provides the tip position, but not the orientation with respect to the sensor. To visualize a 3D model of a non-cylindrical device such as the Emprint ablation needle in the software, Euler angles are necessary.
Apart from a pivot calibration, calibration in surgical tool-tip tracking can also be performed using a calibration device. This is a tracked device that can be calibrated to ensure that the shape, dimensions, position and orientation of the device are known. The 3D printed block used for validation of the calibration accuracy of the ablation needle (Figure 3.8) is such a calibration device. The tip of the instrument to be calibrated is positioned into a divot in the calibration device provided for that purpose. The user then indicates in the corresponding software that the instrument's tip is positioned as such and the tip location of the surgical instrument is calibrated. Commercially available surgical navigation systems such as by CAScination (CAScination AG, Bern, Switzerland) and Brainlab (Brainlab AG,

Munich, Germany) use an optically-tracked calibration device used for the calibration of the tracked instruments, as shown in Figure 3.12. This device is sterilizable and can thus be used for intraoperatively calibration of the length, diameter and vector of a rigid instrument. Moreover, it allows for calibration of a variety of devices. As these devices are commercially only available for optically tracked navigation systems, it could be desirable to create and calibrate a similar device for our EM-tracked system. Unfortunately CustusX does not support this type of calibration so an algorithm should be provided for this purpose.

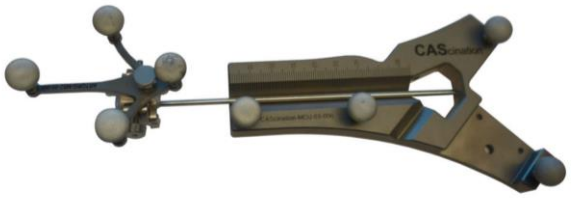

Figure 3.12: Optically tracked calibration device by CAScination [11].

As opposed to most other studies describing navigated ablation, an advantage of our calibration is that it is performed to the point in the antenna from where the microwaves are spread, rather than to the tip of the antenna. As the center of the ablation zone can therefore be navigated to the center of the tumor, this will result in a more accurate ablation. Nonetheless, it should also be noted that the shape of the ablation zone is also dependent on the settings of the power and time, often determined during surgery by the surgeon. The largest diameter of the ablation zone will be located slightly more distal to the antenna when using a higher power and a longer period of ablating, which results in a difference of a few millimeters when changing the settings. The ablation zone reference chart of the Emprint™ needle can be found in Appendix A. To be completely accurate, a different calibration matrix should be created for the different possible settings. In the NKI-AvL open liver ablations are always performed at 100 W, so different calibration matrices should be created for the different settings of time. However, changing the calibration matrix during the process of navigation of the surgery is time consuming and cumbersome.
This could be improved when using an aforementioned calibration device. Instead of calibrating the tip of the ablation needle, the calibration could be set with an offset from the tip corresponding to the settings of the ablation needle. Even more ideal would then be when the settings of the ablation device are directly coupled to the navigation system, so it would not be necessary to set this manually.

At last, during testing we found that needle deflection decreases the accuracy of the navigation as expected. Maximal needle deflection for needles of 14 to 17 Gauge was approximately 5 mm (Figure 3.4). The is in line with our findings, where inaccuracies could reach up to maximal 4 mm when deflecting the 11 Gauge needle. It is difficult to predict the effect of needle deflection during surgery, as tests were now performed using a rigid object that deflects the needle easily but the liver does not provide that level of resistance. Though, it is important that before implementation the surgeons are aware that needle deflection reduces the accuracy of the navigation.

References

1. Wu, W., Xue, Y., Wang, D., Li, X., Xue, J., Duan, S., & Wang, F. (2015). Application of 3D imaging in the real-time US–CT fusion navigation for minimal invasive tumor therapy. *International journal of computer assisted radiology and surgery*, 10(10), 1651-1658.
2. Tomonari, A., Tsuji, K., Yamazaki, H., Aoki, H., Kang, J. H., Kodama, Y., ... & Maguchi, H. (2013). Feasibility of the virtual needle tracking system for percutaneous radiofrequency ablation of hepatocellular carcinoma. *Hepatology Research*, 43(12), 1352-1355.
3. Paolucci, I., Schwalbe, M., Prevost, G. A., Lachenmayer, A., Candinas, D., Weber, S., & Tinguely, P. (2018). Design and implementation of an electromagnetic ultrasound-based

navigation technique for laparoscopic ablation of liver tumors. *Surgical endoscopy*, 32(7), 3410-3419.
4. Wood, B. J., Kruecker, J., Abi-Jaoudeh, N., Locklin, J. K., Levy, E., Xu, S., ... & Venkatesan, A. M. (2010). Navigation systems for ablation. Journal of Vascular and Interventional Radiology, 21(8), S257-S263.
5. CIVCO Medical Solutions. eTRAX™ Needle System System Reference Guide. 2020. URL: https://www.civco.com/assets/documents/ifus/043721.pdf.
6. Jung, E. M., Friedrich, C., Hoffstetter, P., Dendl, L. M., Klebl, F., Agha, A., ... & Schreyer, A. G. (2012). Volume navigation with contrast enhanced ultrasound and image fusion for percutaneous interventions: first results. *PloS one*, 7(3), e33956.
7. De Jong, T. L., Klink, C., Moelker, A., Dankelman, J., & van den Dobbelsteen, J. J. (2018, March). Needle deflection in thermal ablation procedures of liver tumors: a CT image analysis. *In Medical Imaging 2018: Image-Guided Procedures, Robotic Interventions, and Modeling* (Vol. 10576, p. 105761L). International Society for Optics and Photonics.
8. Northern Digital Inc. Electromagnetic Tracking that Supports Minimally Invasive Approaches. 2020. URL: https://www.ndigital.com/products/aurora/.
9. Yaniv, Z. (2015, March). Which pivot calibration?. In *Medical imaging 2015: Image-guided procedures, robotic interventions, and modeling* (Vol. 9415, p. 941527). International Society for Optics and Photonics.
10. Nijkamp, J., Schermers, B., Schmitz, S., de Jonge, S., Kuhlmann, K., van der Heijden, F., ... & Ruers, T. (2016). Comparing position and orientation accuracy of different electromagnetic sensors for tracking during interventions. *International journal of computer assisted radiology and surgery*, 11(8), 1487-1498.
11. Wallach, D., Toporek, G., Weber, S., Bale, R., & Widmann, G. (2014). Comparison of freehand-navigated and aiming device-navigated targeting of liver lesions. *The International Journal of Medical Robotics and Computer Assisted Surgery*, 10(1), 35-43.

Chapter 4

Visualization of navigated ablation

For the implementation of the tracked needle in the surgical navigation workflow, it is important to create views that best assist the surgeon during needle placement. Therefore, software alterations were made in consultation with the hepatobiliary surgeons of our institute. Evaluation of these views was performed using a questionnaire on the user experience.

4.1 Introduction

During navigated liver surgeries, the software used is CustusX (SINTEF, Trondheim, Norway) [1]. CustusX is an open-source research platform for image-guided therapy, with a focus on intraoperative navigation and US imaging. This software allows for custom functionalities to be implemented. It also integrates EM and optical tracking. CustusX provides functionalities for registration and visualization of the preoperative model, intraoperative imaging and tracked surgical instruments during navigation. The graphical user interface can be customized and saved to the preferences of the user.
After registering the preoperative liver model to the intraoperative US images three different views are shown to the surgeon: a real-time US image, an US image with the registered 3D model overlayed and a 3D view of the registered model and the surgical instruments with respect to this model. These views are shown on a screen in proximity to the operating room (OR) table in the view of the surgeon (Figure 4.1). The software is controlled by a technical physician during the surgery.
The view of the US overlayed with the registered 3D model (Figure 4.2) provides direct feedback on the accuracy of the registration, as the anatomy of the 3D model should be overlaying that of the US image, and is therefore an important visualization.
The general 3D view shows the preoperative model with the blood vessels, bile ducts and tumors (that can independently be enabled and disabled in the view) and models of the surgical instruments (pointer, US probe.
A goal of this thesis was to integrate navigated ablation in the current CustusX software, and create a visualization aiding in optimal needle placement.

Figure 4.1: Intra-operative liver navigation setup.

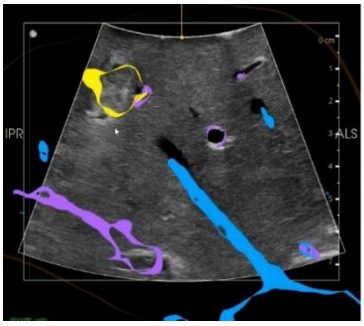

Figure 4.2: US overlay view. The registered 3D model with respect to the intraoperative US imaging. Overlay shows the hepatic vein (blue), portal vein (purple) and tumor (yellow).

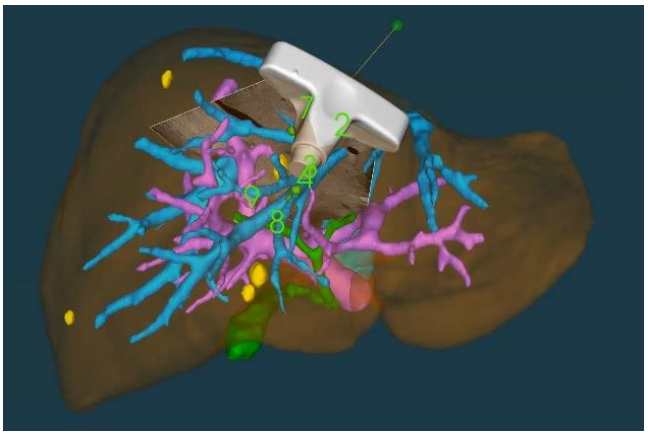

Figure 4.3: General 3D view including a registered model showing the hepatic vein (blue), portal vein (purple), bile ducts and gall bladder (green), tumors (yellow) and the intraoperative US.

4.2 Methods

4.2.1 Generation of the Views

After exploring the visualization methods of current state of the art on needle tracking systems (Chapter 2) and consulting the hepatobiliary surgeons, two views were integrated in the CustusX software.
The first view is a cross-hair (i.e., bullseye) view, where the tumor can be visualized as if looking through the tip of the ablation needle (also mentioned in Section 2.3.3). At the center of the screen, a circle shows when the needle has a direct trajectory to the tumor. Additionally, a ruler shows the distance from the center of the ablation zone to the center of the tumor.
The second view is the general 3D overview with the ablation needle incorporated and a 3D needle trajectory showing where the ablation needle is moving towards when continuing insertion in a straight line with the needle.

For the implementation of navigated ablation in CustusX, a new tool was created in the software. The matrix obtained by the pivot calibration was then saved as a calibration file, to indicate the transformation from the sensor to the center of the ablation zone. The STL file created for the design of the adapter was coupled to the created tool, in order to visualize a 3D model of the needle in the software. Therefore, the origin of the coordinate system of the STL file was set to be at the exact same location as the center of the ablation area on the antenna, as these origins will then correspond in the general 3D view of the software (Figure 4.4).

Figure 4.4: Origin of STL file ablation needle placed at the center of the ablating area on the antenna.

CustusX has the built-in functionality "tool view", which uses a fixed camera on the tip of the tool and a "moving" patient, useful for integration of the bullseye view. Pivoting calibration solely results in a translation, as rotation cannot be determined with this method. Therefore, without the rotation calibration, the orientation for the tool view corresponded to the orientation of the sensor rather than following the direction of the ablation antenna.
The tool view of CustusX always considers the camera view to be in the direction of the z-axis. Thus, a transformation was necessary to change the orientation of the tool, to ensure that the orientation of the z-axis would be aligned in the direction of the needle.
The calibration of the orientation was acquired using the calibration block as a reference, as the needle was positioned in a known orientation with respect to the block (Figure 4.5a and Figure 4.5b). Consequently, the coordinate system of the ablation needle was then visualized in CustusX. As shown in Figure 4.5c, the tool view now does not follow the direction of the ablation antenna. In order to change the orientation of this view, the general 3D view is used. Here, the coordinate systems are visualized and for each axis (x,y,z), an angle α can be obtained to rotate the axis accordingly (Figure 4.5d). The angle α was calculated in ImageJ (Fiji, version 2017, https://imagej.net/Fiji/Downloads) [2]. These angles for the three axes were then converted to rotation matrices, which were then multiplied with each other. The obtained rotation was then combined with the translation obtained by the pivot calibration to finally result in the desired transformation matrix and correct tool view (Figure 4.5e).
To enable the bullseye and a distance measure from needle to tumor, so-called metrics were created in the software. The bullseye is created using a donut metric and the distance measure could be provided by including a distance metric.

For the general 3D overview the STL orientation had to be altered to correspond with the actual orientation of the ablation needle (Figure 4.5f). This was done by reorienting the STL file in 3D Slicer based on calculation of the necessary rotation for each axis using ImageJ. Finally, a sphere metric on the ablation needle was created in the CustusX software to show the predicted ablation zone.

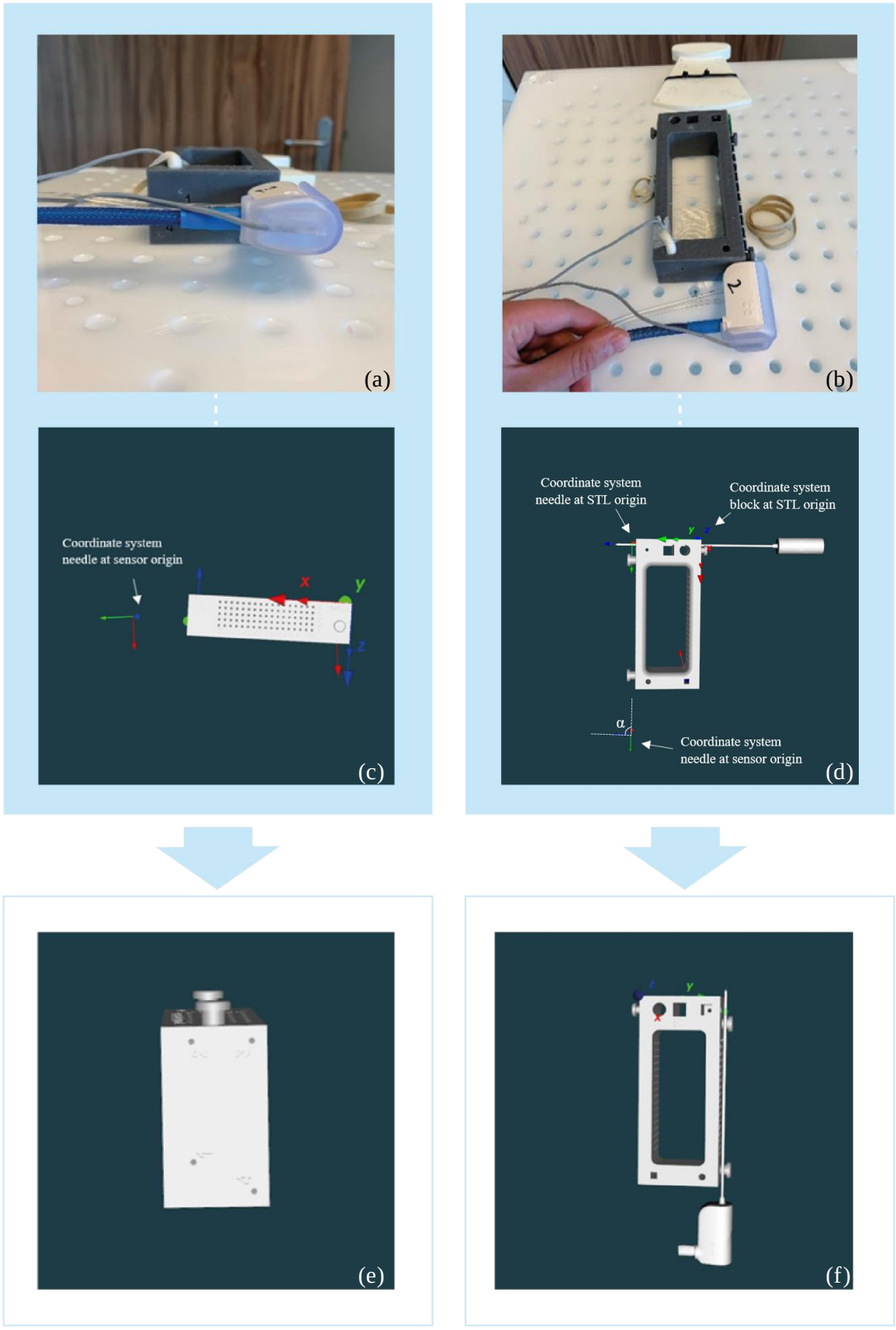

Figure 4.5: Calibration of the orientation of the ablation needle in CustusX software using a calibrated block. The ablation needle is positioned with respect to the block (a, b). Without the orientation calibration, the tool view was oriented in the z-direction of the sensor coordinate system (c) and the STL in the 3D view followed the coordinate system at the STL origin (d). After orientation calibration the tool view (e) and the general 3D view (f) were corrected.

4.2.2 Usability Evaluation

To assist the surgeons in accurately placing the needle, ease of software use and user friendliness are necessary. To evaluate those features, a questionnaire was designed (Appendix B).
The first ten questions regarded the workflow of navigated liver ablation, which view the surgeons preferred most and if the navigation was of added value to the surgeon.
The other questions are based on the System Usability Scale (SUS) [3]. According to [3], measures of usability should cover three important items: effectiveness, efficiency and satisfaction (was the surgeons experience satisfactory). The SUS covers these three items by making a statement where the answers consist of a five-point scale going from 1 (strongly disagree) to 5 (strongly agree). For each individual question, a maximum of 4 points can be acquired. For items 1,3,5,7, and 9 the score is the scale position minus 1. For items 2,4,6,8 and 10, the score is 5 minus the scale position. Finally, to calculate the SUS score, the sum of the scores were multiplied by 2.5, which results in a score between 0 and 100. A SUS score above a 68 would be considered above average and anything below 68 is below average. The advantages of using the SUS are that it is short, systematic and validated.
Finally, the last seven questions directly compare the navigation technology with the conventional liver ablation procedure. Scores range from 1-5; where an experience of the new system scored with a 3 is similar to the conventional setting and a score below 3 is considered a negative experience. This method directly shows whether the innovation leads to a positive or negative experience for its user.
The system was tested during a liver ablation and the surgeons were shown the two views: the bullseye view and the general 3D view. However, needle placement was not performed through the navigation, as this requires further validation. After the surgery, the surgeons were asked to fill in the questionnaires to evaluate their opinion of the system.

4.3 Results

The bullseye view is shown in Figure 4.6. In this view, the surgeon is virtually looking through the tip of the needle to the preoperative model. Features that are shown in this view are:

- the tumor shown in yellow, modelled based on the preoperative imaging;
- a point shown with a red 'T' indicating the tumor center;
- a circle (bullseye) shown in red, indicating whether a direct trajectory to the tumor is available;
- and a distance in millimeters from the center of the ablation zone on the antenna to the center of the tumor (point T).

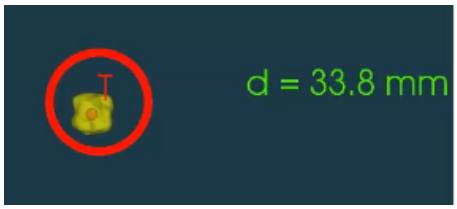

Figure 4.6: Bullseye view for navigated needle placement.

The general 3D view that can be shown during navigated microwave ablation is shown in Figure 4.7. Features that are shown in this view are:

- the ablation needle shown in grey;
- the registered liver model (hepatic vein in blue, portal vein in purple, bile ducts in green, tumor(s) in yellow;
- the ablation zone, displayed as a green sphere, with its center on the point of calibration.

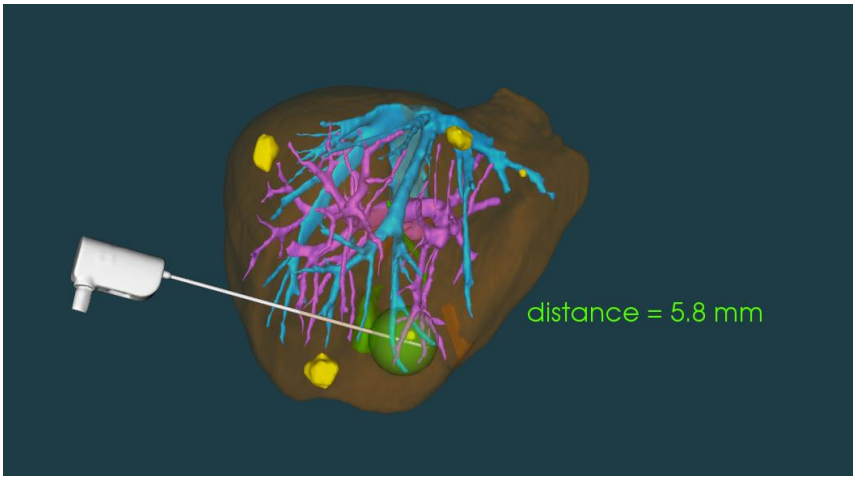

Figure 4.7: General 3D view of navigated ablation.

In CustusX, it is also possible to change the color of the tumors ablated. In this case, if a patient has multiple tumors to be ablated, it is possible to keep track of which lesion has already been treated.

The system was tested in clinical settings and the evaluation form on the user experience was compiled independently by three hepatobiliary surgeons. The answers to the general questions on user experience can be found in Figure 4.8. All surgeons preferred the bullseye view compared to the general 3D view, as they found it easier to interpret during needle placement. No problems were encountered during the workflow and the navigation was found to be an addition in needle placement.
The mean SUS score for the three surgeons was 65%, of which the average results per question can be found in Figure 4.9. This means the system is quite complex and some of the functionalities were difficult to use. Nevertheless, most points in the SUS were lost due to the fact that navigation is currently not possible without the support of a technical person. Moreover, the surgeons responded that they did not require extensive training before using the system and they wanted to use the system more regularly. The overall experience of the surgeons with the navigation technology for liver ablation was more positive than the conventional method of ablation (Figure 4.9). Navigation could reduce the complexity of the ablation, helping in localizing tumor(s), reducing complications, obtaining negative ablation margins and it increases certainty in decisions and actions.

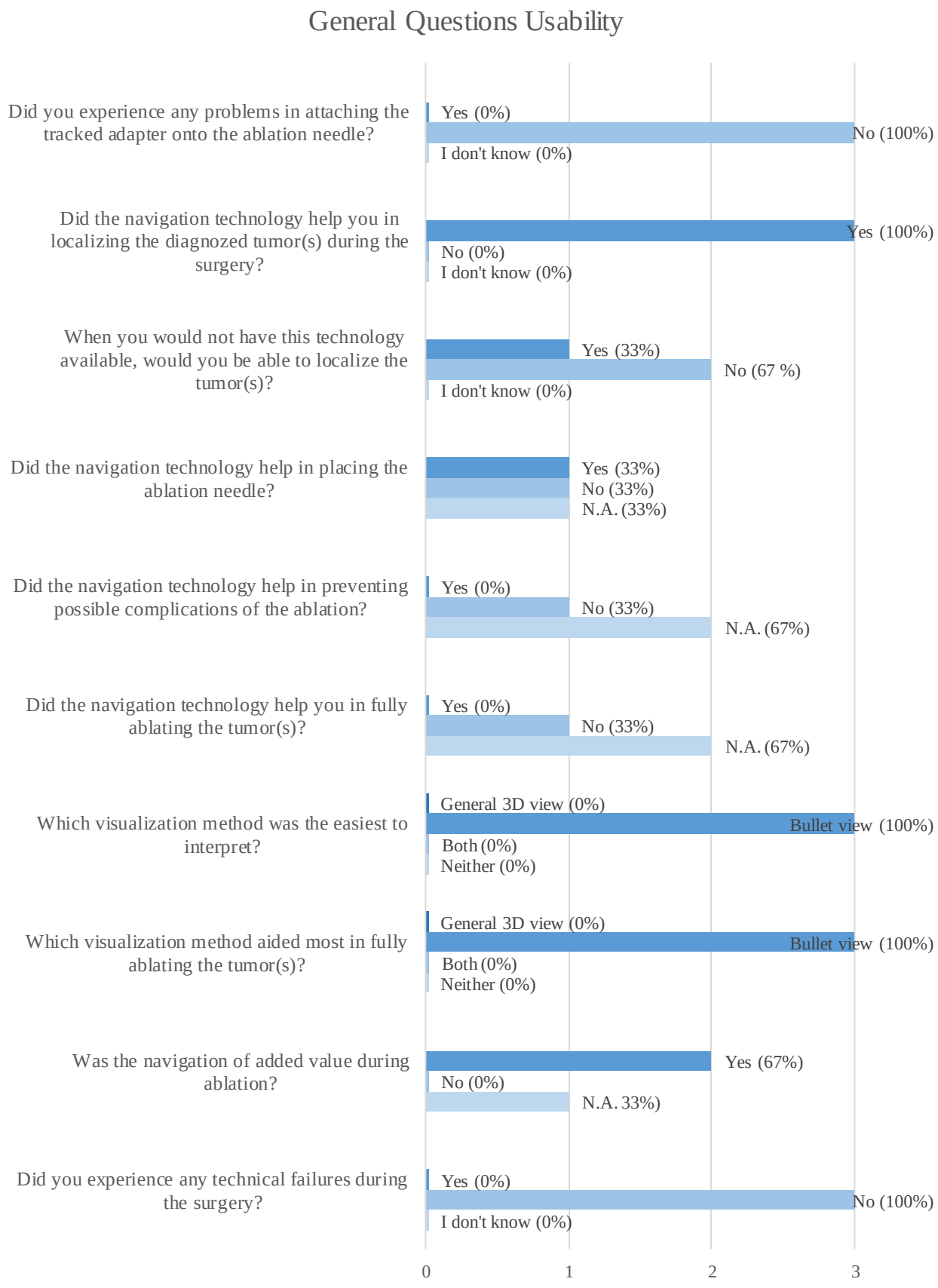

Figure 4.8: Results of the general questions on usability of navigated liver ablation.

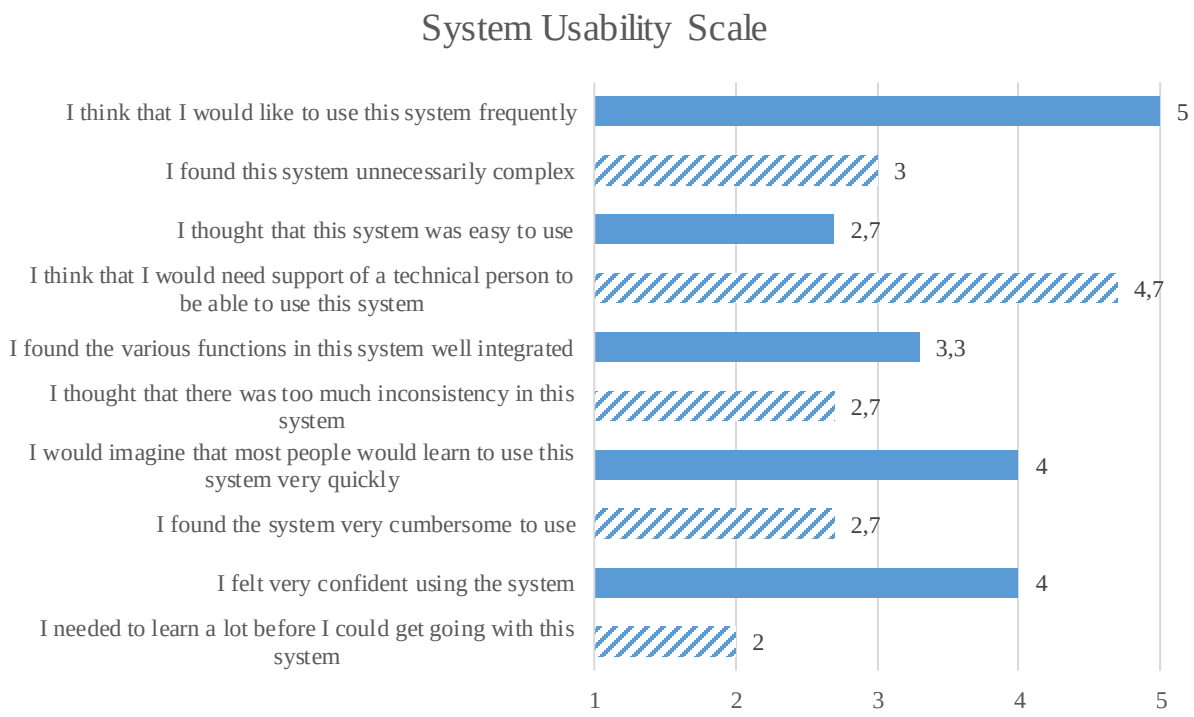

Figure 4.9: Results of the System Usability Scale. For an optimal score, the questions indicated with solid bars are scored a 5 and the patterned bars scored a 1.

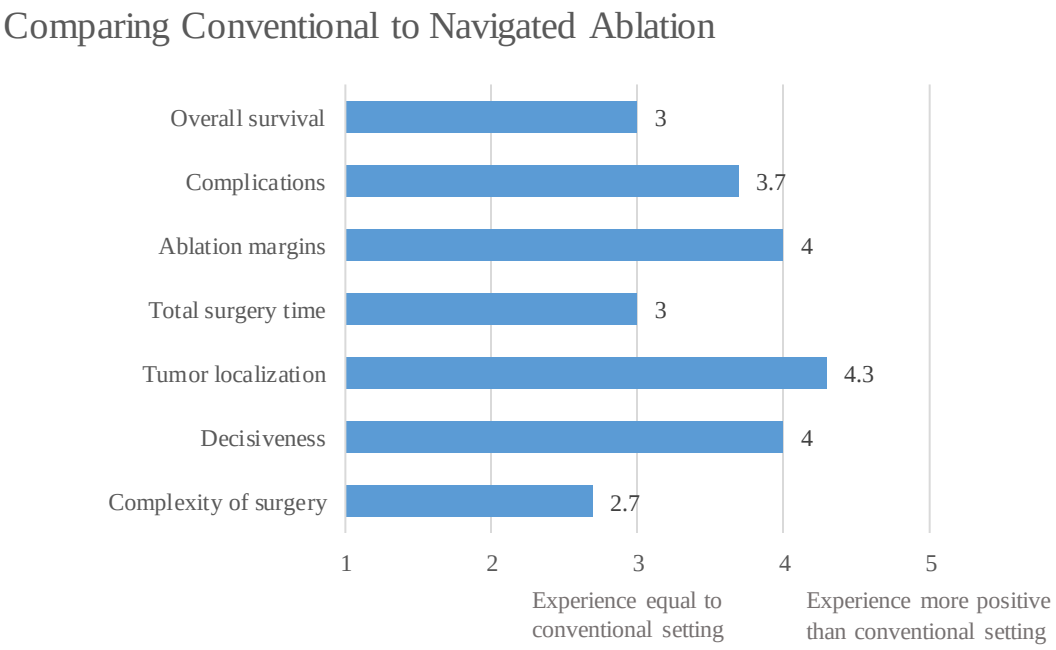

Figure 4.10: Results of comparison between the conventional method of open liver ablation to navigated ablation.

4.4 Discussion

Two different views for navigated liver ablation were created and tested by three hepatobiliary surgeons during open liver ablation. The views were evaluated using an evaluation form on the user experience. When comparing the system with the conventional technique of ablation, navigation results in an increased decisiveness and a better tumor localization. Nevertheless, the system obtained a SUS of 65 which is not yet sufficiently high, when considering the threshold of 68.
This can be explained by the fact that despite surgeons preferred the bullseye view for guidance in needle placement, there is a learning curve to familiarize with the view. The bullseye view currently shows a bullseye view in the center of the screen in which the tumor should be guided. This can be difficult to interpret, since in reality, the tumor is standing still and the needle is moving, so one would expect the bullseye to move instead of the tumor. However, this arises other problems, as the bullseye could also appear behind or on the side of the tumor, depending on the needle location. When working with the system, the surgeons did show to quickly adapt to the interpretation of the bullseye view.

The most important limitations arise from the restrictions the CustusX software carries, even though there are extensive possibilities in creating custom views in the software.
Ideally, it would be possible to show the bullseye view together with the US overlay. This is not possible in the current CustusX version, as for the US overlay, the US has to be marked as an "active tool" in the software. For the bullseye view, this "active tool" should be the ablation needle. In this version of CustusX, it is not possible to mark two active tools at the same time. Therefore, it is currently required to switch between the views in order to see them at the same time. A different version of the software was created for the NKI-AvL by the developers of CustusX to show both views simultaneously. Yet, there are still bugs, which currently prevent the possibility of implementing this during surgery.
Moreover, it is only possible to visualize an absolute distance measure. When using the bullseye view, which is in 2D, it would be favorable to have an indication of the depth of the needle with respect to the center of the tumor instead of an absolute distance. The bullseye view gives an overview of the offset of the direction of the ablation needle but not the depth of the needle. However, as an absolute distance is provided to the surgeon, it does not show whether the needle is inserted too superficial or too deep into the tissue. An additional view, i.e., the general 3D overview, can provide the surgeon with this information.
As shown in Figure 4.7, it is possible to show a green sphere with the size of the ablation zone. When this completely overlaps the tumor, the tumor would be completely ablated. However, the size of the ablation zone is dependent on the settings of the power and time of the ablation device. Currently, the size of the sphere has to be manually adjusted. Ideally, the ablation device is coupled to the navigation system. Then, when the time and power of the device are set, the correct ablation zone appears in the navigation software.
Projection of the needle trajectory in the general 3D view but especially in the US overlay image is desired and in the future this should be integrated in the navigation software. This would also provide real-time information on the amount of needle bending, since the actual needle as well as the projected trajectory are then visible in the US view.
At this moment, the research group working on the implementation of navigated liver surgery is developing their own navigation software, to overcome current limitations of the CustusX software.

Important feedback of one of the surgeons was that, since currently US is still crucial visualization for needle placement, it is very hard to focus on two extra views. It is only possible to process two different inputs at the same time. Therefore, only one view in addition to US imaging is. As shown in the user experience evaluation, the bullseye view is preferred over the general 3D view. When in the future US is no longer required in addition to navigation, the general 3D view could be provided as an additional view to the bullseye view.

The process of calibration of the needle for the bullseye view within the software requires several steps and experience. Yet, since the adapter and its calibration are validated and robust after multiple sterilization cycles, this process only has to be performed once. The calibration relies on calculation of the angles using ImageJ, which can result in some slight inaccuracies. However, these inaccuracies cannot be noticed with the unaided eye, since calculation of the angle in ImageJ is performed under a large zoom factor. Needle placement will therefore not be affected and clinical consequences are absent. Also, distance measure is based on the pivot calibration, which will therefore be very accurate, when there is no bending of the needle. Alternatively to this process, a calibration device could be created for calibration of the tip position and orientation of the ablation needle.

In conclusion, surgical navigated liver ablation can be performed using the CustusX software. The first clinical tests shows promising results and a more positive experience than the conventional method of liver ablation. Nonetheless, improvements should be made in the expected software at the NKI-AvL to improve the usability of the visualization methods.

References

1. Askeland, C., Solberg, O. V., Bakeng, J. B. L., Reinertsen, I., Tangen, G. A., Hofstad, E. F., ... & Lindseth, F. (2016). CustusX: an open-source research platform for image-guided therapy. *International journal of computer assisted radiology and surgery*, 11(4), 505-519.
2. Rasband, W.S., ImageJ, U. S. National Institutes of Health, Bethesda, Maryland, USA, https://imagej.nih.gov/ij/, 1997-2018.
3. Brooke, J. (1996). Sus: a "quick and dirty' usability. *Usability evaluation in industry*, 189.
4. Likert, R. (1932). A technique for the measurement of attitude scales.

Chapter 5

Towards clinical implementation

A method for intraoperative validation for navigated liver ablation was developed. This was tested in a multimodal anthropomorphic liver phantom, which proved the system to determine the location of the tip of the ablation needle with a mean accuracy of 2.2 mm. Thereafter, in vivo experiments are required to determine the accuracy of the system during its intraoperative application.

5.1 Introduction

The method for navigated liver ablation proposed in the previous chapters can be clinically implemented. Nevertheless, this method first requires in vivo validation. This chapter describes a method for intraoperative validation of the created workflow for navigated liver ablation and testing in a liver phantom. Figure 5.1 provides an overview on possible sources of errors in navigated liver ablation. The registration error and influence of organ deformation on the accuracy of the navigation are important factors but do not fall within the scope of this research. To validate the developed method for navigated ablation, the contribution of the needle calibration error and the needle deformation to the overall targeting error is of particular interest.

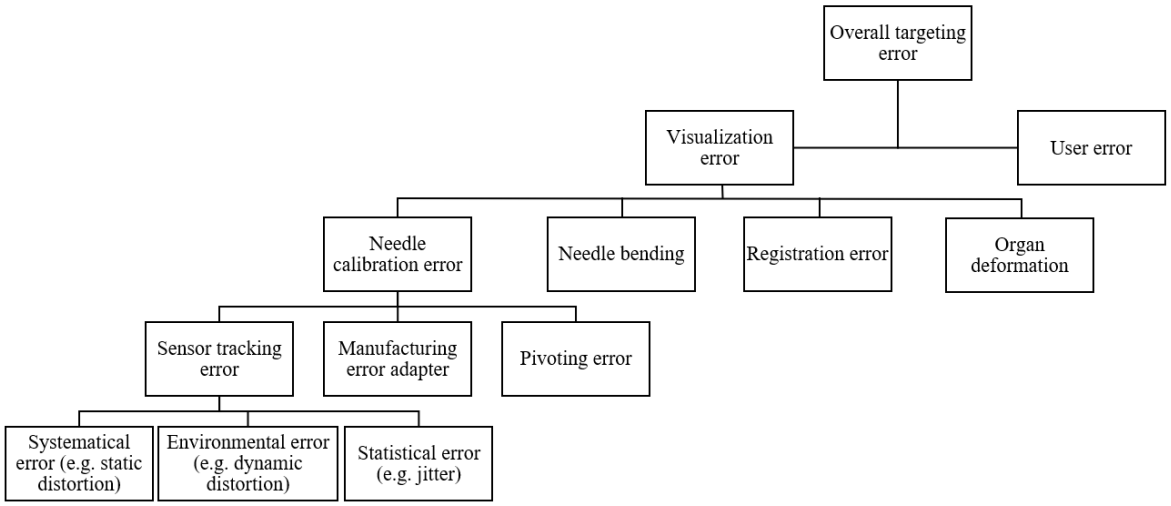

Figure 5.1: Possible sources of errors in navigated liver ablation.

Validation of navigated liver ablation in an in vivo setting is challenging, since there are limited options for obtaining information on the exact location of the tip of the ablation needle when it is inserted in the organ. This results in very few studies analysing the tracking accuracy of navigated liver ablation. Information of the tip position in the liver can be obtained using intraoperative imaging, such as CT or US. Due to the fact that it is the standard imaging modality in and does not make use of ionizing radiation, US is preferable for this purpose.
When the surgeon is provided with additional intraoperative US which can show the ablation needle, this can be visually compared to the location of the ablation needle in the navigation. Another means of validation is proposed by Paolucci et al. [1]. In this study, a 3D US scan of the target lesion and the positioned ablation needle is acquired. The target positioning error (TPE), i.e., the distance from the tip of the ablation antenna to the lesion can therefore be calculated. In this phantom study, a TPE of 4.2 mm was achieved for electromagnetic navigated laparoscopic liver ablation. A comparable method could be used for validating the navigated liver ablation system at the NKI-AvL. However, instead of calculating the TPE, we are interested in comparing the tip location in the US volume to the tip as shown in the CustusX software.

5.2 Methods

A multimodal liver phantom was created using a method developed by Ruitenbeek [2]. This phantom consists of mimicked tissue of the liver parenchyma, veins and tumors. The veins and tumor are fabricated using silicone sealant. For the parenchyma, a mix of candle gel and 10 grams of magnesium oxide was heated in a pan and stirred using magnetic stirring bars. A shallow layer of the mix was poured into a plastic container, placed at an angle of approximately 30° and cooled. The tumor and vessel were placed on top and the remaining candle gel was poured onto them. After the phantom was cooled and removed from the container (Figure 5.2a) a CT scan of the phantom was acquired and a 3D model was made based on this scan (Figure 5.2b).

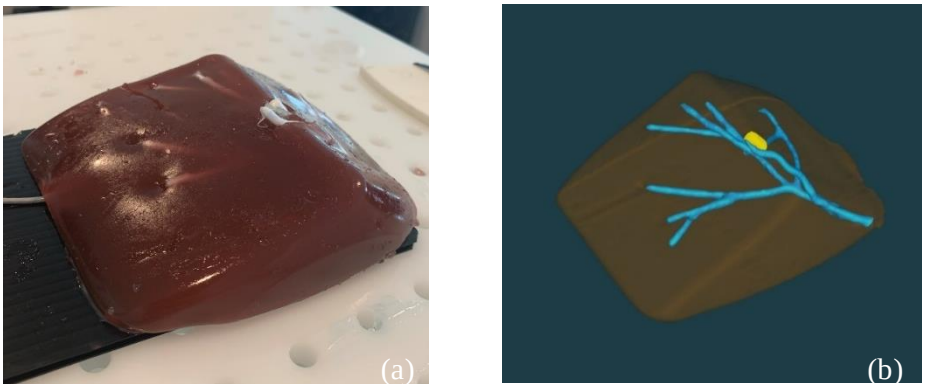

Figure 5.2: Multimodal anthropomorphic liver phantom (a) and its 3D model (b).

The liver phantom was used to validate whether the tip location computed from the calibrated adapter attached to the ablation needle corresponds with the true position of the needle tip when placed in the tumor.

The phantom was placed into the EM field of the tabletop field generator. A sensor was placed underneath the phantom as a reference sensor (patient tracker) and the 3D model was loaded into the CustusX software. A landmark-based registration was performed based on vessel bifurcations. Subsequently, the ablation needle was placed in the liver phantom and a tracked US sweep was made of the liver volume including the tip of the ablation antenna. Then, the needle was fixated at the same position and the positions and orientation of the sensors of the ablation needle, US and the reference sensor were recorded in NDI Track. This was performed three times, where the ablation needle was placed in different locations inside the liver phantom.

After data acquisition, the US volume is loaded into 3D Slicer. The needle is then segmented and the position of the needle tip in the US in determined by placement of a fiducial marker, which will be mentioned as Tip_{US} further on (Figure 5.3). This is assumed to be the true location of the tip, as US is considered the standard image guidance during needle placement.

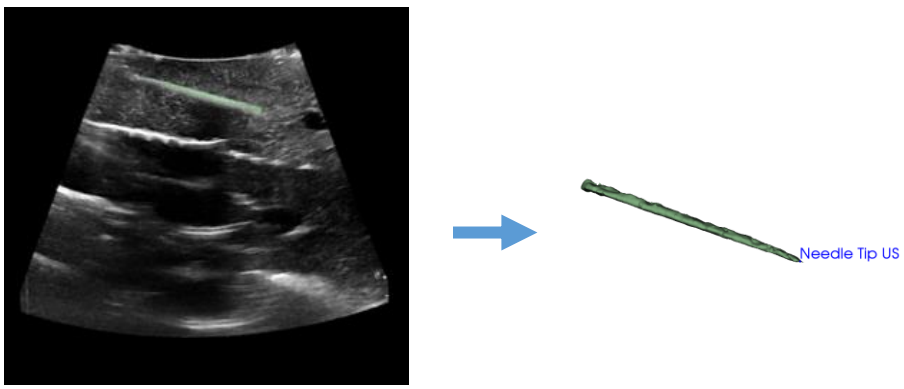

Figure 5.3: Determining position needle tip in US volume.

The positions and orientations of the sensors recorded were NDI Track were loaded into MATLAB (The MathWorks, Natick, MA, USA, version 2021a, https://nl.mathworks.com/). To calculate $Tip_{Adapter}$, the position and orientation of the adapter sensor with respect to the EM field (${}^{EM}T_{Abl}$) was multiplied with the calibration matrix obtained from the pivot calibration (${}^{Abl}T_{Tip}$). In order to compare the two tip locations, $Tip_{Adapter}$ was registered to Tip_{US}, since these positions were not defined in the same coordinate system. The US volume is expressed in the coordinate system of the patient tracker, for which the $Tip_{Adapter}$ was transformed using ${}^{PT}T_{EM}$. Finally, as the US volume is registered to the preoperative imaging, this registration (${}^{MR}T_{EM} \cdot {}^{EM}T_{US}$) was performed on $Tip_{Adapter}$, resulting the two tip locations to be in the same coordinate system (Formula 5.1). Figure 5.4 shows an overview of the steps of the aforementioned registration.

$$ {}^{MR}T_{Abl} = {}^{MR}T_{EM} \cdot {}^{EM}T_{US} \cdot {}^{PT}T_{EM} \cdot {}^{EM}T_{Abl} \cdot {}^{Abl}T_{Tip} \tag{5.1} $$

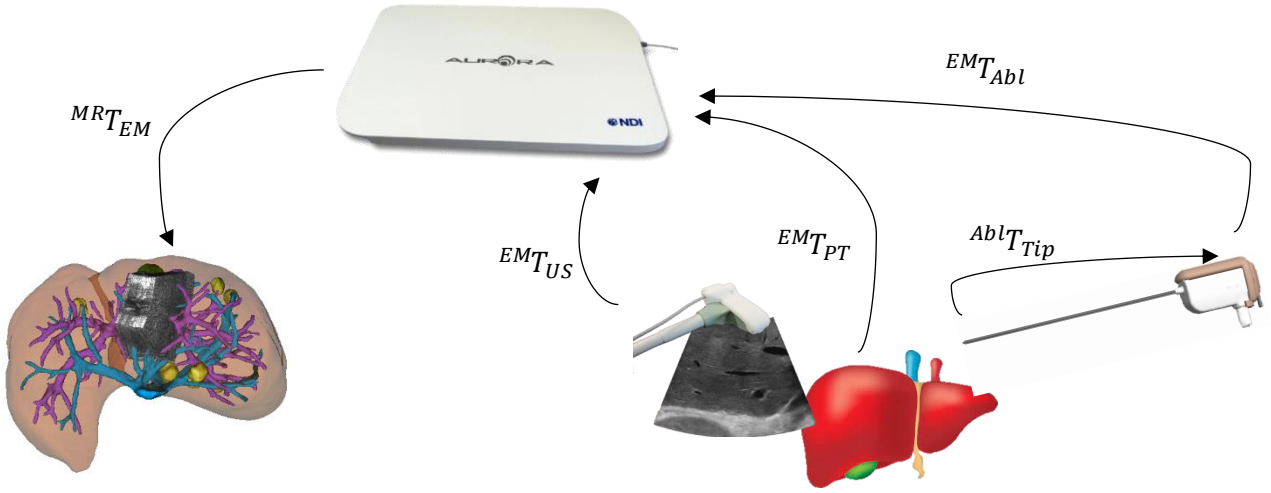

Figure 5.4: Overview of steps taken for registration from adapter sensor to intra-operative US.

The Euclidean distance between Tip_{US} and $Tip_{Adapter}$ was then calculated. Since 3D Slicer is expressed as a left-handed coordinate system, as opposed to the right-handed NDI system, $Tip_{Adapter}$ was converted using the matrix shown in Figure 5.5.

$$ \begin{matrix} -1 & 0 & 0 & 0 \\ 0 & -1 & 0 & 0 \\ 0 & 0 & 1 & 0 \\ 0 & 0 & 0 & 1 \end{matrix} $$

Figure 5.5: Matrix for conversion from left-handed to right-handed coordinate system.

5.3 Results

The ablation needle was placed in three different locations of the liver phantom. The accuracy of the calibration was tested by comparing the tip of the ablation needle from the calibrated adapter to the tip in the US volume, expressed in the preoperative imaging coordinate system. The Euclidean distances are shown in Figure 5.6. The mean Euclidean distance of these phantom tests was 2.2 mm.

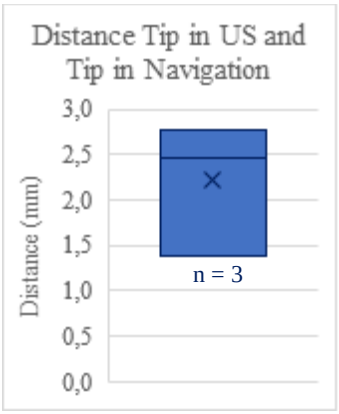

Figure 5.6: Distance between ablation needle tip in US and in navigation software in liver phantom (n = 3).

5.4 Discussion

Apart from determining the TPE, current literature does not describe a method for calculating the tracking accuracy of the needle tip during in vivo navigated liver ablation. This chapter describes a method to accomplish this by determining the contribution of the needle calibration error and needle deflection to the overall targeting error for an open navigated liver ablation system. This method was tested in a phantom setting, where tracking of the tip of the ablation antenna could be performed with an accuracy of 2.2 mm.
The advantage of determining the tracking accuracy during needle placement, is that the only increase of the surgery time is as a result of taking an US sweep of the tumor volume together with the tip of the ablation antenna, which takes approximately ten seconds. Subsequently, the surgeon starts ablation so the needle is held still, since during ablation it is difficult to visualize on US the tumor location. As MWA induces gas bubbles in the ablation zone due to the heating of the tissue to near the boiling temperature, the incident acoustic waves cause hyperechoic regions on the US [3]. So, while the needle is held still, the positions and orientation of the sensors are recorded in NDI Track. After ablation of the tumor, which is generally performed for approximately five minutes, all necessary data is acquired.
Apart from determining the tracking accuracy, it is also possible to determine the TPE, i.e., the distance from the center of the tumor to the center of the ablation zone from the acquired 3D US volume. When the method for navigated liver ablation is validated and final needle placement can be performed based on the navigation, the TPE could provide insight in whether the navigation actually results in more accurate needle placement compared to the conventional workflow of liver ablation.

During the development of this validation method, several critical choices are made that will be substantiated below.
First, IOUS was used to determine the true location of the tip of the ablation needle. A disadvantage however is that the needle causes scattering within the image which can make it challenging to place the fiducial marker exactly at the tip of the antenna. IOUS is the standard imaging modality used for liver ablation and therefore used as gold standard.
Secondly, in the proposed validation method, NDI Track is used to determine the needle tip location when inserted into the tumor. This is not done using the CustusX software, since it is not possible to save the 3D scene shown in the software. Multiplication of the sensor location and calibration matrix of the adapter provides the exact tip location as shown in CustusX.
Additionally, instead of comparing the relationship between the needle tip in the navigation software and in the US volume, alternatively one could investigate the relation between the needle tip to the target lesion, i.e., the TPE, in the software and in the US volume. In that case the inaccuracy of registration is added to the final error. This is not ideal, as we want to quantify the inaccuracies solely

of the tracking of the ablation antenna. However, it should be kept in mind that the final navigation, including the distance measure from the ablation antenna to the center of the tumor as shown in the navigation software, is dependent on the accuracy of the calibration, as well as other factors such as the registration error and organ deformation (Figure 5.1).
There are some limitations to the proposed validation method. In some regions of the liver (e.g., the cranial part of segment II and VII) it can be challenging to perform an US sweep without deforming the liver, since these regions are difficult to reach with the US probe. This is especially the case, when displacement of the liver needs to be prevented. In these cases, it will not be possible to validate the navigation method as an US sweep is required.
Also, during this method the accuracy of the navigation system is only determined when the needle is already placed. During this stage, needle bending is expected to be minimal, since the surgeon attempts to hold the needle in the same position during the ablation. Yet, the amount of needle deflection could be different during needle positioning. Additional information on this can be supplied by the general 3D view, where the US image is also provided to the surgeon. Figure 5.7 shows images from the first surgery performed with the navigated liver ablation setup. When the antenna is deflected, this decreases the accuracy of the navigation resulting in the model of the antenna to not overlay with the needle in the US image (Figure 5.7a). When no pressure is carried out on the ablation needle, it overlays with the antenna as shown in the US image (Figure 5.7b).

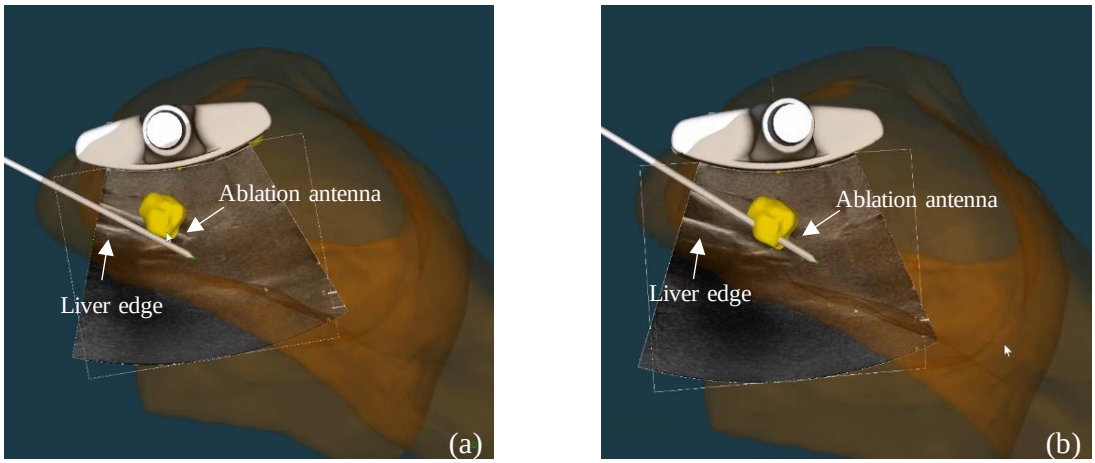

Figure 5.7: General 3D view of the navigated liver ablation in CustusX during needle placement; (a) needle is deflected which results in an inaccurate overlay on the US image, (b) the needle model corresponds with its alias in the US image.

Even though navigated liver ablation was clinically implemented and data acquisition was performed, validation of this navigation was not achievable as recording of the sensor coordinates in NDI Track was not performed correctly. Within the approval by the Medical Ethics Review Committee (METC) for the N18ULN study, consent was obtained to evaluate feasibility and accuracy of real-time electromagnetic tracking of MWA needles during ablations of liver lesions in open surgery in vivo in 28 patients. This will be the next step in this research. Throughout the clinical study, the system will be validated and not yet used for final needle placement which will be performed using IOUS.

References

1. Paolucci, I., Schwalbe, M., Prevost, G. A., Lachenmayer, A., Candinas, D., Weber, S., & Tinguely, P. (2018). Design and implementation of an electromagnetic ultrasound-based navigation technique for laparoscopic ablation of liver tumors. *Surgical endoscopy*, 32(7), 3410-3419.

2. Ruitenbeek, H.C. Development of a multimodal anthropomorphic liver phantom for the improvement of navigated tumour treatment. 2019. URL: http://essay.utwente.nl/81528/.
3. Zhou, Z., Wu, S., Wang, C. Y., Ma, H. Y., Lin, C. C., & Tsui, P. H. (2015). Monitoring radiofrequency ablation using real-time ultrasound Nakagami imaging combined with frequency and temporal compounding techniques. *PLoS One*, *10*(2), e0118030.

Chapter 6

Conclusions and future recommendations

Open liver ablation is a well-accepted treatment for liver malignancies. For complete ablation of the tumor, the ablation volume should encompass the tumor volume including a 5-10 mm margin to take into account potential micro-metastases around the visible tumor [1]. To achieve complete tumor ablation, precise intraoperative localization of the tumor and accurate needle placement are crucial. This can be challenging due to the technical limitations of intraoperative image guidance during liver ablation. Surgical navigation can potentially solve this. The objective of this thesis was therefore to develop and validate a complete surgical workflow for EM tracked open liver ablation.

An adapter for tracking of the Emprint microwave ablation needle was created and validated for usability, sterilizability and reproducibility of the calibration. The ablation needle can be tracked with a comparable accuracy to that of the Aurora surgical pointer. Moreover, the calibration of the adapter is robust after multiple runs of sterilization.
Additionally, the user interface of the software currently used for navigated liver surgeries was adapted, in order to integrate navigated liver ablation. The complete navigation system and workflow was tested intraoperatively. Afterwards, a survey on the user evaluation amongst the hepatobiliary surgeons was conducted. This showed that the bullseye view showing a cross-hair of the tumor as if you are looking through the tip of the ablation needle, is preferred most.

Experiments performed in a liver phantom showed promising results, with a tracking accuracy of 2.2 mm when compared to US. Future research should provide further insights in the accuracy of the in vivo tracking of the ablation needle. Intraoperative validation will be performed on 28 patients during navigated liver ablation. A tool tracking accuracy of approximately 2 mm in vivo would be satisfactory, especially because this also includes the errors that can arise during analyzation of the US volume, due to scattering of the needle in the imaging. Ideally, when the system is fully validated and this accuracy can be achieved, US will no longer be necessary for needle placement.
Generally, only small tumors (Ø<3 cm) are considered eligible for ablations, where ablation zones are usually 4-5 cm in diameter [2]. Therefore, for navigated liver ablation systems, an overall accuracy of 10 mm at the target lesion is in general considered clinically acceptable and useful for decision making [3]. Ideally, we would obtain an accuracy below 3-5 mm with our system, as this would allow the surgeons to actually change the procedure based on the information provided by the navigation.

A large contributor to the final accuracy of the navigation is the registration accuracy which is challenging in a deformable organ such as the liver. These registration methods are especially important in the case of vanishing lesions, where the tumor is not visible on US. Accordingly, the navigation software can visualize the initial location of the tumor during the time of preoperative imaging (CT or MRI), which could be of help during liver ablation. Still, in cases where the tumor is visible on US, navigation could result in an increased certainty during needle insertion, avoidance of large vessels and biliary ducts and a more exact placement of the antenna.
In these cases, a registration might not be necessary and direct delineation of the tumor on the IOUS could result in a more accurate navigation. Preferably, the tumor would be automatically segmented in the 3D US volume, to obtain a 3D model of the tumor. Consequently, the ablation needle could be navigated to the center of this segmented tumor. Using deep learning, it is currently attempted to create an automatic tumor segmentation algorithm at the NKI-AvL. Nevertheless, this has not been successful until now, as tumor segmentation in US imaging can be very challenging as the appearance of tumor in US can vary in size, shape and they can appear either hyper-, hypo or even isoechoic. Another option is described by a recent study using semi-automatic tumor segmentation in US imaging [4]. In this method, the largest diameter of the tumor is found using the IOUS and the center of the tumor is marked.

Then, the approximate size of the tumor is selected, where a sphere segmentation is created indicating the tumor. This segmentation can be optimized by further indicating areas that have to be added or removed from the segmentation. In the future, it is advised to look into these tumor segmentation methods in order to bypass the necessity of a registration for navigated liver ablation.

Even though navigated ablation is possible using the current software and created views, some software alterations are still required for an optimal navigation workflow. Initially, the new version of CustusX could be used when this is debugged by the developers which will allow to show two active tools at the same time. Therefore, the US overlay view and bullseye view could be shown simultaneously.
For an optimal visualization, the views of navigated ablation will need to be integrated in the navigation software, which is currently being developed at the NKI-AvL. In this, the most important alteration will be the visualization of the needle trajectory in the US image, aiding the surgeon in identifying the most optimal path for needle insertion.

At last, when validation of the open navigated liver ablation system is completed, this could in the future be adapted to a laparoscopic setting. Laparoscopic liver surgery is increasingly performed throughout the past years. Expected advantages of laparoscopic liver surgery compared to the open approach are reduced blood loss, shorter hospital stay and less complications. Moreover, in some cases patients are not eligible for open surgery but can be operated laparoscopically, due to their medical comorbidities or poor performance status. Shifting towards a minimal invasive surgery for the case of navigated liver ablation arises in additional challenges to overcome before implementation. For instance, the use of a longer ablation needle results in higher chance of needle deflection, the surgeon has to operate with lack of haptic feedback of the liver tissue when guiding the instrument and the laparoscopic ultrasound (LUS) has to be tracked and calibrated.

In conclusion, a workflow for navigated liver ablation was developed and the first in vivo tests with the system were promising. In the future, navigation could lead to more accurate ablations and lower chance of disease recurrence. A clinical study will now be performed at the NKI-AvL to validate the method for clinical implementation.

References

1. Mahnken, A. H., Ricke, J., & Wilhelm, K. E. (Eds.). (2009). *CT-and MR-guided Interventions in Radiology* (Vol. 22). New York: Springer.
2. Wells, S. A., Hinshaw, J. L., Lubner, M. G., Ziemlewicz, T. J., Brace, C. L., & Lee, F. T. (2015). Liver ablation: best practice. *Radiologic Clinics*, 53(5), 933-971.
3. Fusaglia, M., Tinguely, P., Banz, V., Weber, S., & Lu, H. (2016). A novel ultrasound-based registration for image-guided laparoscopic liver ablation. *Surgical innovation*, 23(4), 397-406.
4. Paolucci, I., Sandu, R. M., Sahli, L., Prevost, G. A., Storni, F., Candinas, D., ... & Lachenmayer, A. (2019). Ultrasound Based Planning and Navigation for Non-Anatomical Liver Resections–An Ex-Vivo Study. *IEEE Open Journal of Engineering in Medicine and Biology*, 1, 3-8.

Appendix A: Ablation Zone Reference Chart Emprint™

Ablation width	45W			75W			100W			150W		
A (cm)	B (cm)	Time (MM:SS)	C (cm)	B (cm)	Time (MM:SS)	C (cm)	B (cm)	Time (MM:SS)	C (cm)	B (cm)	Time (MM:SS)	C (cm)
2.3				2.6	1:30	0.2	2.7	1:00	0.2			
2.4	2.5	2:30	0.2									
2.5	2.6	3:00	0.2	2.8	2:00	0.3						
2.6	2.7	3:30	0.2				3.0	1:30	0.3			
2.7	2.8	4:30	0.3	2.9	2:30	0.3						
2.8	3.0	6:00	0.3	3.1	3:00	0.3	3.2	2:00	0.4	3.5	1:00	0.5
2.9	3.1	8:00	0.4	3.2	4:00	0.4	3.3	2:30	0.4			
3.0	3.2	10:00	0.4	3.3	4:30	0.4	3.4	3:00	0.5			
3.1				3.4	6:00	0.5	3.5	3:30	0.5	3.7	1:30	0.6
3.2				3.6	8:30	0.5	3.7	4:30	0.5	3.9	2:00	0.6
3.3				3.6	10:00	0.5	3.8	5:30	0.6			
3.4							3.9	7:30	0.6	4.1	2:30	0.7
3.5							4.0	10:00	0.7	4.2	3:00	0.7
3.6										4.3	3:30	0.7
3.7										4.5	4:30	0.8
3.8										4.6	6:00	0.8
3.9										4.7	8:00	0.9
4.0										4.8	10:00	0.9

Appendix B: Form User Experience Navigated Liver Ablation

Onderzoek naar de gebruikerservaring van de navigatietechnologie tijdens een open leverablatie

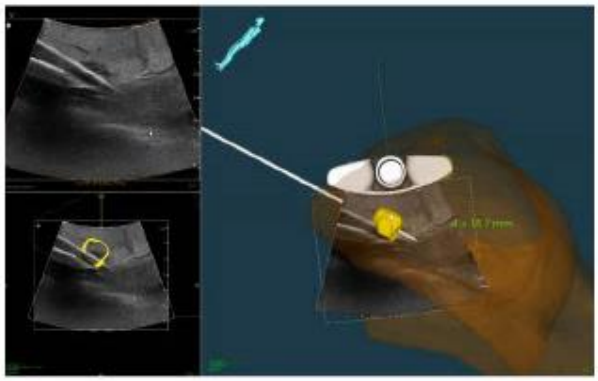

In te vullen door onderzoeker / implementatieteam

Studie ID: N18ULN

Corresponderend bij patiënt studie ID: _____

Ingevuld door (naam arts): _____

Datum operatie: ___-___- 20____

ANTONI VAN LEEUWENHOEK
NEDERLANDS KANKER INSTITUUT

Versie 1.1 – innovatieve technologie

Toelichting
Beste gebruiker,
U heeft gebruik gemaakt van het in het AVL ontwikkelde navigatiesysteem tijdens een open leverablatie. We willen hiervoor zo goed mogelijk in kaart brengen hoe dit wordt ervaren door de gebruiker en wat voor effecten deze technologie met zich mee brengt. Vandaar dat we u willen vragen de volgende vragenlijst in te vullen. Mocht u nog extra opmerkingen hebben over de technologie, de voorbereiding en/of het proces eromheen is hier aan het einde van de vragenlijst ruimte voor.
Mocht er iets niet duidelijk zijn kunt u contact opnemen met Karin Olthof (ka.olthof@nki.nl) of Jasper Smit (j.smit@nki.nl; telefoon 1283)
Bij voorbaat hartelijk dank voor uw tijd en moeite!

1. **Heeft u problemen ondervonden bij het bevestigen van de getrackte adapter op de ablatienaald?**
   - ☐ Ja, namelijk: ……
   - ☐ Nee

2. **Heeft de navigatietechnologie u geholpen bij het lokaliseren van de gediagnosticeerde tumor(en) tijdens de operatie?**
   - ☐ Ja, volledig
   - ☐ Ja, voornamelijk bij …… van de ……. **gediagnosticeerde tumor(en)**
   - ☐ Nee

3. **Wanneer u deze technologie niet tot uw beschikking had, had u dan ook de gediagnosticeerde tumor(en) kunnen lokaliseren?**
   - ☐ Ja, volledig
   - ☐ Ja, maar alleen bij …… van de ……**gediagnosticeerde tumor(en)**
   - ☐ Nee

4. **Heeft de navigatietechnologie geholpen bij het plaatsen van de ablatienaald?**
   - ☐ Ja, namelijk bij: ……
   - ☐ Nee
   - ☐ Weet ik niet

5. **Heeft de navigatietechnologie geholpen bij het voorkomen van eventuele complicaties van de ablatie?**
   - ☐ Ja, namelijk bij: ……
   - ☐ Nee
   - ☐ Weet ik niet

6. **Heeft de navigatietechnologie u geholpen bij het volledig ableren van de tumor(en)?**
   - ☐ Ja
   - ☐ Nee
   - ☐ Weet ik niet

Onderstaand ziet u een afbeelding van twee visualisatie methoden in de navigatiesoftware: (a) 3D overview ten op zichte van de echo probe, (b) bullet view van de tumor in geel gevisualiseerd ten op zichte van de ablatienaald.

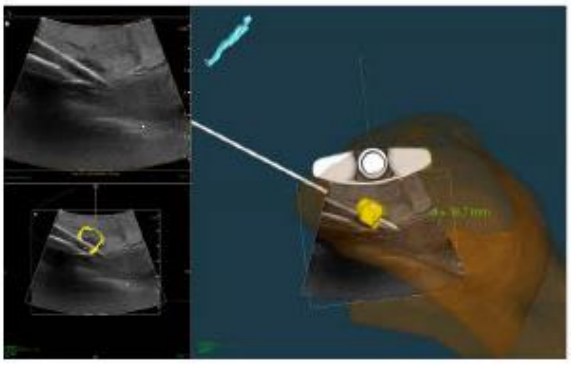

(a)

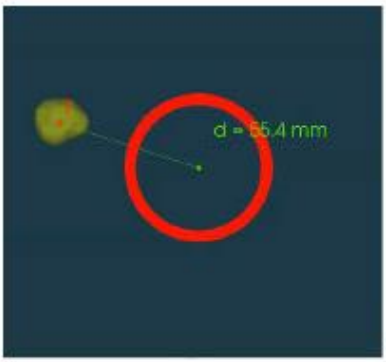

(b)

7. **Welke visualisatie methode vond u het gemakkelijkst te interpreteren?**
   - ☐ Methode a
   - ☐ Methode b
   - ☐ Beide
   - ☐ Geen van beide

8. **Welke visualisatie methode heeft u het meest geholpen in het volledig ableren van de tumor(en)?**
   - ☐ Methode a
   - ☐ Methode b
   - ☐ Beide
   - ☐ Geen van beide

9. **Was de navigatie tijdens de ablatie een aanvulling?**
   - ☐ Nee
   - ☐ Ja, zou u uit kunnen leggen waarom?

   .....

   .....

10. **Heeft u tijdens deze operatie technische storingen ervaren?** *Zo ja, zou u deze zo goed mogelijk kunnen beschrijven?*
    - ☐ Nee
    - ☐ Ja, ...

      .....

Hieronder volgen 10 algemene vragen met betrekking tot de gebruiksvriendelijkheid van de beeld gestuurde technologie die u tijdens deze operatie heeft gebruikt. Houd in gedachte dat onderstaande vragen met betrekking tot de **genavigeerde ablatie** zijn en dus niet de navigatie in zijn geheel.
Ter interpretatie: wanneer gesproken wordt over integratie en tegenstrijdigheden (vragen 14 en 15) van het systeem heeft dit betrekking op de mate waarin de visualisatie correspondeert met de werkelijkheid op het scherm. Dus, is de navigatie ablatienaald en het gebruik hiervan goed geïntegreerd in de visualisatie en in hoeverre laat dit tegenstrijdigheden zien met de werkelijkheid.

		Sterk Mee oneens				Sterk Mee eens
10	**Ik denk dat ik dit systeem graag regelmatig wil gebruiken**					
		1	2	3	4	5
11	**Ik vond het systeem onnodig complex**					
		1	2	3	4	5
12	**Ik vond het systeem makkelijk te gebruiken**					
		1	2	3	4	5
13	**Ik denk dat ik ondersteuning nodig heb van een technisch persoon om dit systeem te kunnen gebruiken**					
		1	2	3	4	5
14	**Ik vond dat de verschillende functies in dit systeem erg goed geïntegreerd zijn**					
		1	2	3	4	5
15	**Ik vond dat er teveel tegenstrijdigheden in het systeem zaten**					
		1	2	3	4	5
16	**Ik kan me voorstellen dat de meeste mensen zeer snel leren om dit systeem te gebruiken**					
		1	2	3	4	5
17	**Ik vond het systeem erg omslachtig in gebruik**					
		1	2	3	4	5
18	**Ik voelde me erg vertrouwd met het systeem**					
		1	2	3	4	5
19	**Ik moest erg veel leren voordat ik aan de gang kon gaan met dit systeem**					
		1	2	3	4	5

Hieronder volgen nog 6 vragen waarbij u de navigatietechnologie vergelijkt met de conventionele methode van ablatie.
Scoor de verschillende aandachtspunten van een operatie met navigatietechniek ten opzichte van een conventionele operatie zonder navigatietechniek. Ga er daarbij vanuit dat de conventionele techniek zonder navigatie een 3 scoort. Dus bij een negatievere ervaring, scoor je lager dan 3, bij geen verschil een 3 en wanneer het beter wordt ervaren hoger dan 3.

		Ervaring negatiever		Gelijk aan conventionele setting		Ervaring positiever
20	**Effectiviteit van de operatie: overleving**					
		1	2	3	4	5
21	**Effectiviteit van de operatie: complicaties**					
		1	2	3	4	5
22	**Effectiviteit van de operatie: ablatie marges**					
		1	2	3	4	5
23	**Efficiëntie van de operatie: totale tijd**					
		1	2	3	4	5
24	**Efficiëntie van de operatie: lokalisatie van de tumor**					
		1	2	3	4	5
25	**Zekerheid in beslissingen en handelen**					
		1	2	3	4	5
26	**Complexiteit van de operatie**					
		1	2	3	4	5

27. Mocht u eventuele extra opmerkingen hebben over de navigatietechnologie zelf of het proces eromheen, kunt u deze hieronder beschrijven.

.....

.....

.....

.....